

Article

Energy Transition in Urban Water Infrastructures towards Sustainable Cities

Helena M. Ramos ^{1,*}, Modesto Pérez-Sánchez ^{2,*}, Prajwal S. M. Guruprasad ³, Armando Carravetta ⁴, Alban Kuriqi ¹, Oscar E. Coronado-Hernández ⁵, João F. P. Fernandes ⁶, Paulo J. Costa Branco ⁶ and Petra Amparo López-Jiménez ²

¹ Civil Engineering Research and Innovation for Sustainability (CERIS), Instituto Superior Técnico, Department of Civil Engineering, Architecture and Environment, University of Lisbon, 1049-001 Lisbon, Portugal; alban.kuriqi@tecnico.ulisboa.pt

² Hydraulic Engineering and Environmental Department, Universitat Politècnica de València, 46022 Valencia, Spain; palopez@upv.es

³ Energy Technologies Dual Degree Program, Instituto Superior Técnico and Karlsruhe Institute of Technology, CERIS at IST, 1049-001 Lisbon, Portugal; prajwalshandilya6227@gmail.com

⁴ Department of Civil, Structure and Environmental Engineering, Università di Napoli Federico II, Via Claudio, 21, 80125 Napoli, Italy; armando.carravetta@unina.it

⁵ Instituto de Hidráulica y Saneamiento Ambiental, Universidad de Cartagena, Cartagena 130001, Colombia; ocoronadoh@unicartagena.edu.co

⁶ IDMEC, Instituto Superior Técnico, Universidade de Lisboa, 1049-001 Lisboa, Portugal; joao.f.p.fernandes@tecnico.ulisbos.pt (J.F.P.F.); pbranco@tecnico.ulisbos.pt (P.J.C.B.)

* Correspondence: helena.ramos@tecnico.ulisboa.pt or hramos.ist@gmail.com (H.M.R.); mopesan1@upv.es (M.P.-S.)

Abstract: The world's water infrastructures suffer from inefficiencies, such as high energy consumption and water losses due to inadequate management practices and feeble pressure regulation, leading to frequent water and energy losses. This strains vital water and energy resources, especially in the face of the worsening challenges of climate change and population growth. A novel method is presented that integrates micro-hydropower plants, with pumps as turbines (PATs), in the water network in the city of Funchal. Sensitivity analyses evaluated the microgrid's response to variations in the cost of energy components, showing favorable outcomes with positive net present value (NPV). PV solar and micro-wind turbines installed exclusively at the selected PRV sites within the Funchal hydro grid generate a combined 153 and 55 MWh/year, respectively, supplementing the 406 MWh/year generated by PATs. It should be noted that PATs consistently have the lowest cost of electricity (LCOE), confirming their economic viability and efficiency across different scenarios, even after accounting for reductions in alternative energy sources and grid infrastructure costs.

Keywords: water infrastructures; hybrid energy solutions; water networks; EPANET; HOMER; PAT; solar PV; wind; LCOE

Citation: Ramos, H.M.;

Pérez-Sánchez, M.; Carravetta, A.; Kuriqi, A.; Coronado-Hernández, O.E.; Fernandes, J.F.P.; Branco, P.J.C.; López-Jiménez, P.A. Energy Transition in Urban Water Infrastructures towards Sustainable Cities. *Water* **2024**, *16*, 504. <https://doi.org/10.3390/w16030504>

Academic Editor: Wencheng Guo

Received: 17 January 2024

Revised: 31 January 2024

Accepted: 2 February 2024

Published: 4 February 2024



Copyright: © 2024 by the authors. Licensee MDPI, Basel, Switzerland. This article is an open access article distributed under the terms and conditions of the Creative Commons Attribution (CC BY) license (<https://creativecommons.org/licenses/by/4.0/>).

1. Introduction

By managing natural resources, society exerts significant pressure on the natural environment [1]. There is a threat of systemic collapse. As a result, many industrialized nations have begun implementing green energy strategies, reaching over 10% of total energy production [2]. The projection of energy consumption, especially in regions under significant urbanization pressure and associated carbon dioxide emissions, poses a formidable challenge to society [3]. The acceleration of economic development and rising standards of living have made energy security a top priority for policy makers worldwide [4].

This predicament requires a city to take innovative approaches to resource management to improve the quality of life for its residents. Achieving these goals is consistent with the imperative to minimize resource use, leading to increased sustainability efforts [5]. Water research has provided clear evidence on the global dimension of the water challenge and the role of humans as a chief force shaping the global water cycle [6,7]. Water infrastructures, in particular, are characterized by high energy consumption, ranging from 0.2 to 4.08 kWh/m³ [8]. This energy is mainly obtained from pumping stations. It includes the energy required to perform various processes and distribution activities. Renewable resources such as solar, wind, and hydropower offer viable alternatives for providing this energy and reducing dependence on non-renewable sources [9].

Using renewable energy systems involves integrating hybrid pumped storage, photovoltaic, and wind turbine systems in conjunction with battery storage [10]. The synergistic use of these technologies enables water utilities to operate their water systems independently of the conventional grid infrastructure [11], in which the pumped hydro-storage is a real infrastructure to manage the renewable production [12].

Numerous research studies have used heuristic methods to develop flexible solutions for hybrid system optimization [13]. Parameters such as temperature, wind speed, and solar radiation significantly impact the optimization of these hybrid systems, as found by [14]. Moreover, a comprehensive review of different techniques for hybrid system optimization has been given in [15]. For this purpose, various algorithms have been used, including genetic algorithms for solar and wind systems in Hong Kong [16], particle swarm optimization for power generation in Rafsanjan (Iran) ranging from 42 to 80 kW [17], and an imperialistic competition algorithm for a 1450 kW hybrid system in Pulau Perhentian (Malaysia) [18]. Harmony search methods were used by [19] to optimize the components of the hybrid system with a power of 1 kW.

Researchers [20] formulated an approach for optimal sizing of distributed power generation by photovoltaic and diesel generator systems using energy management and size optimization through a new approach for an islanding solution. The gray wolf optimization method was used to determine the optimal number of PV panels, wind turbines, and battery banks while considering the minimum annual cost [21]. Another optimization of hybrid systems focusing on minimizing electricity costs was performed using the firefly-inspired algorithm [22]. In contrast, harmony search methods were used to minimize life cycle costs in a hybrid system in Ardabil (Iran) [23]. Evolutionary algorithms and artificial bee swarm optimization were also used to optimize various hybrid systems, such as the 7 kW system in Rafsanjan [24] and the 5 kW system [25].

On the other hand, examples of hybrid system sizing using the big bang–big crunch method were presented in [26], with an optimized power target of 3715 kW. In [27], using HOMER software, a performance analysis of off-grid hybrid power systems in remote areas was carried out, minimizing the net present cost and CO₂ emissions. In addition, HOMER was used to optimize hydro systems with hydropower and photovoltaic plants in Lisbon (Portugal) [28]. The authors of [29] developed an optimized methodology using simulated annealing for hybrid systems involving photovoltaic and micro-hydropower systems with pumps as turbines (PATs), achieving an annual reduction of 2838 tons of CO₂ emissions and 553 MWh of energy generated from non-renewable sources in Spanish irrigation systems. The feasibility of similar systems in remote cities, such as the Bahamas, was investigated in a case study by [30].

Integrating these technologies into water management is essential to improve the water–energy nexus. This aligns with the Sustainable Development Goals (SDGs) and enables adaptation to the challenges of climate change while reducing greenhouse gas emissions [31]. Numerous studies highlight how implementing operational strategies can significantly improve the sustainability of water distribution networks while optimizing energy management [31].

Following the references above, energy communities can use associations, cooperatives, partnerships, nonprofit organizations, or small/medium businesses to facilitate citizen participation and joint investment in energy assets [32]. This collaborative approach contributes to a decarbonized and more flexible energy system, as energy communities can act as a unified entity that can access renewable energy markets in different combinations and at a smaller scale [33]. By upgrading the water sector, an essential service for the population, energy communities can contribute to grid flexibility through adaptive demand reduction mechanisms [34].

In summary, energy communities offer an opportunity to reshape how society perceives and integrates essential variables such as water and energy satisfaction. By harnessing available renewable energy sources, citizens can actively participate in the energy transition, resulting in significant benefits for all. Pressure-reducing valves (PRVs) are used in water distribution networks to ensure standardization and regulation of pressure, dividing the water network into pressure zones according to topographical conditions. The operation of PRVs results in a localized loss of pressure and, thus, a loss of hydraulic energy due to a lower outlet pressure. PRVs generate controlled pressure and flow zones where an efficient management of water losses becomes possible, allowing for faster detection and response [35–37].

Pumps as turbines (PATs) provide an alternative means of pressure control in water distribution networks (WDNs) and increase system efficiency and flexibility. However, the main disadvantage of PATs is the lack of flow device control, which leads to suboptimal efficiency when flow rates fluctuate. For WDNs, flow and head pattern fluctuations can reduce overall energy production due to low efficiency at partial load and the inability to provide the required head for suitable operational conditions. In general, manufacturers do not provide the characteristics of PATs, which is one of the biggest challenges for their application.

Under stable operating conditions, pressure-reducing valves (PRVs) and PATs exhibit similar behavior. Therefore, PATs are a viable alternative for generating sustainable energy at low cost. Despite the drawbacks and challenges of implementing PATs, they offer a compelling alternative for harnessing hydropower and improving system efficiency. This results in reduced dependence on other energy sources and induces lower operating costs. Integrating PATs into WDNs can improve water, energy, and cost management in intelligent water grids and is an important step toward developing future smart cities [38–44].

The addition of strategies to improve the sustainability of water systems is crucial to reach the zero-emission balance [45–47]. Hence, this research proposes a new strategy that includes different optimized methods, both hydraulic and energetic, that allow for improving the management of water distribution systems to analyze the possibility of combining different renewable systems to meet energy needs in small energy communities [48,49]. The development of this research enables the establishment of a green management proposal, which allows water managers the development of new strategies to improve sustainability in the water sector [50].

2. Materials and Methods

The methodology used in this study includes the use of water networks that supply water to local communities, focusing on identifying possible optimal locations for pressure-reducing valves (PRVs), controlling the pressure in the network, for the recovery of water energy (e.g., pumps as turbines—PATs) to generate hydropower. Next, (i) hydraulic simulation (ii) can be used to identify the implementation of PATs and (iii) the energy simulation with complementarity between other renewable sources to generate an optimal hybrid small energy solution that (iv) allows for the analysis of microgrids in an economical way through the best combination of renewable systems (Figure 1).

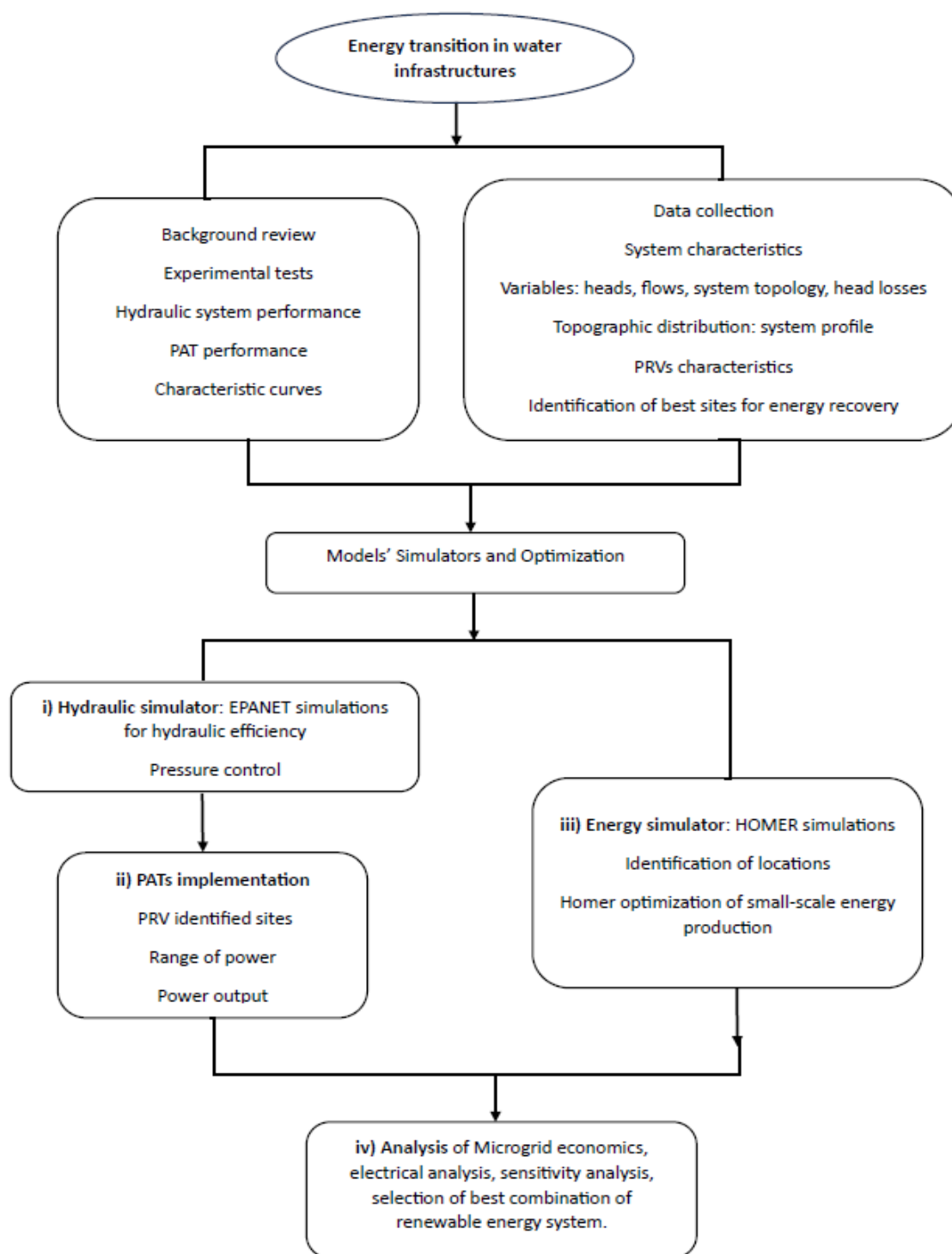


Figure 1. Flow chart of the proposed integrated methodology.

2.1. Hydraulic Model Simulator

The hydraulic simulation methods used in the analysis of water distribution networks rely on the EPANET model (or equivalent) developed by the U.S. Environmental Protection Agency (EPA) (Figure 2). This model allows for both static simulations and simulations over time so that hydraulic behavior and flow and pressure distribution throughout the network can be evaluated.

The EPANET simulator (2.2) is widely known and considered one of the most widely used software applications for water system simulation. EPANET uses the “gradient method” to derive equations governing the principles of continuity, energy conservation, and the relationship between flow and pressure drop, all of which characterize hydraulic equilibrium within a piping system. The continuity of flow at a node is governed by Equation (1), while Equation (2) establishes the relationship between flow and pressure drop in a pipeline segment from node i to j . Equation (3) specifies the demand for each branch of the pipeline network.

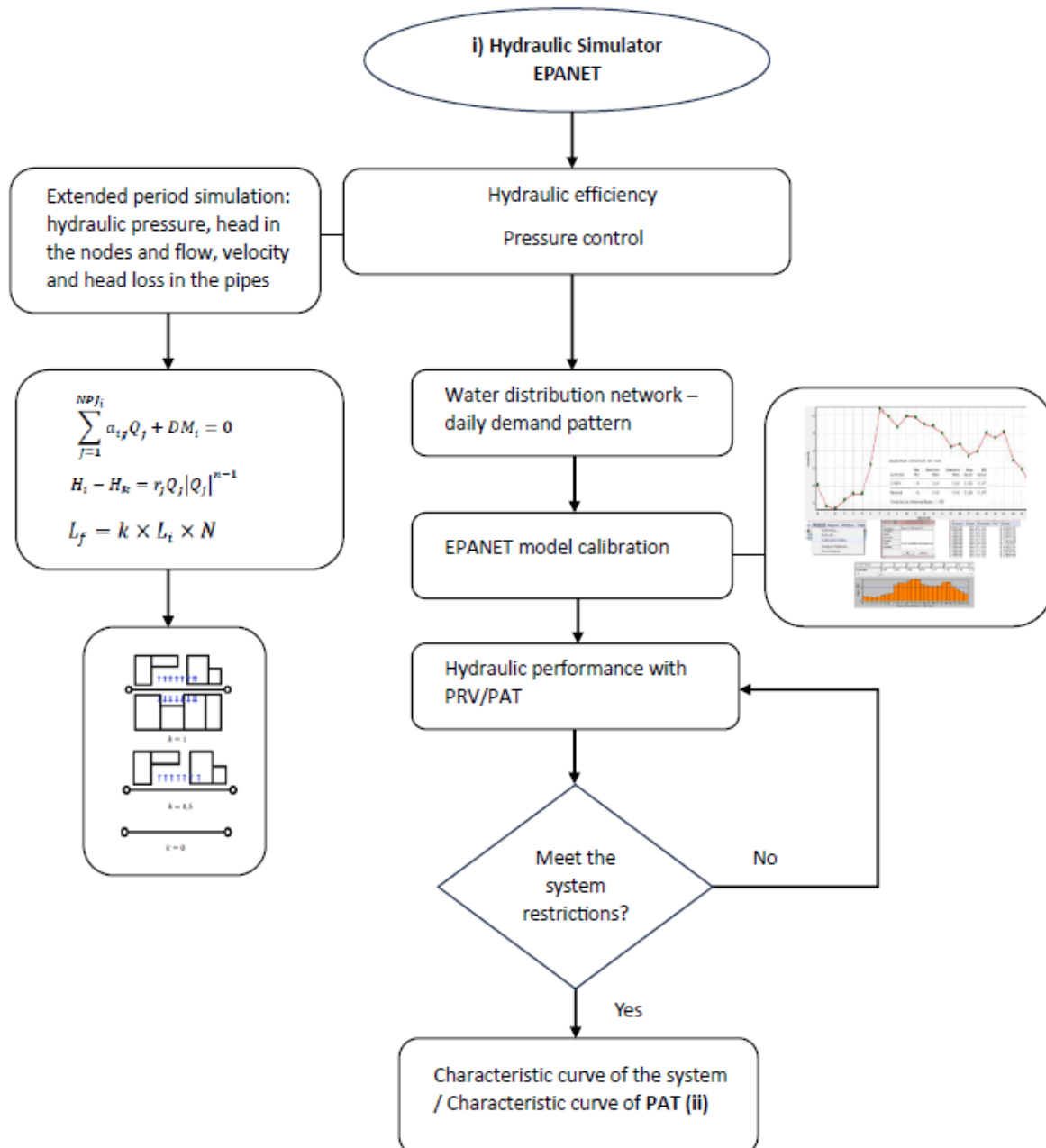


Figure 2. Hydraulic simulator methodology.

$$\sum_j a_{ij} Q_{ij} + D_i = 0 \tag{1}$$

for $i = 1, \dots, N$

$$H_i - H_k = h_{ik} = rQ_{ij}^{n-1} \quad (2)$$

$$L_f = k \cdot L_i \cdot N \quad (3)$$

where D_i is the demand in each node (by convention, the flow that arrives at the node is positive) (L/s), H_i is the nodal head (m), h is the head loss (m), r is the resistance coefficient, Q is the flow rate (L/s), n is the flow estimation orifice leak exponent, L_f is the fictitious pipe length, L is the real pipe length, and N is the number of building floors. The coefficient k depends on the line service, whether on both sides, at just one side, or with no service. Thereby, knowing the head of the fixed nodes, it is possible to obtain the heads, H_i , and flows, Q_{ij} , of the network that satisfies Equations (1)–(3). The water resource calculation involves multiplying the peak flow observed at each valve by the corresponding hourly demand curve.

2.2. Energy Recovery with PATs

Implementing pump-as-turbine (PAT) systems in energy recovery involves identifying key parameters, such as flow rate and available head, to estimate power output. In addition, pressure-reducing valves (PRVs) are critical in maintaining pressure control within the network. Installation of PAT systems is defined in terms of various modes of operation, including no control (NR); hydraulic control (HR), which includes additional valves in the main line and PAT bypass; energy control (ER), which is achieved by variable operating speed (VOS) of the PAT impeller; or a combination of both (HER) (as shown in Figures 3–5).

Once the locations for the pressure-reducing valves (PRVs) are identified, a characteristic curve of the installation (CCI) is generated based on the measured inlet and outlet pressures at the PRV nodes. This CCI illustrates the relationship between flow rate and available head within the hydraulic system. An appropriate characteristic curve for a pump as turbine (CCPAT) is then selected that matches the hydraulic characteristics of the network. In defining the CCPAT, various maximum heads are established to match local pressure conditions and ensure optimal utilization for power generation. The CCPAT curves are carefully matched to the flow rate and head in the system to maximize the extraction of available hydroelectric energy. The point where the characteristic curve of the system intersects with the characteristic curve of the PAT defines the operating point of the turbine.

To simulate the implementation of pump-as-turbine (PAT) systems, the pressure-reducing valves (PRVs) in the EPANET model are replaced by general-purpose valves associated with the corresponding turbine characteristics. Then, following the principles of hydraulic similarity, characteristic curves are defined for different speeds (in an energy regulation mode). The relationship between electric power and hydraulic power generates several efficiency points that facilitate the preparation of an efficiency analysis.

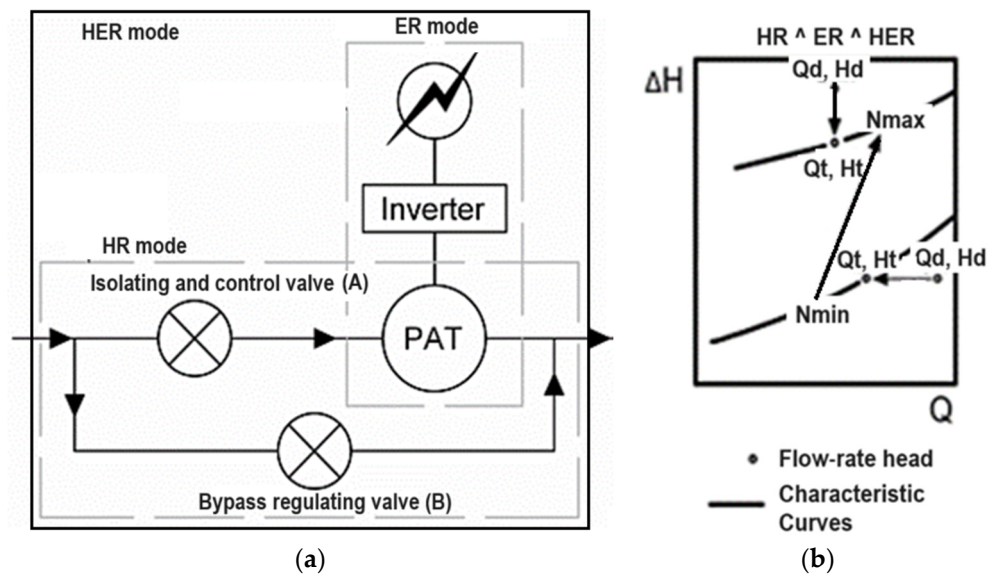


Figure 4. Scheme of a PAT in a pipe system (a), with hydraulic and/or electrical regulation (HR, ER, HER) (b).

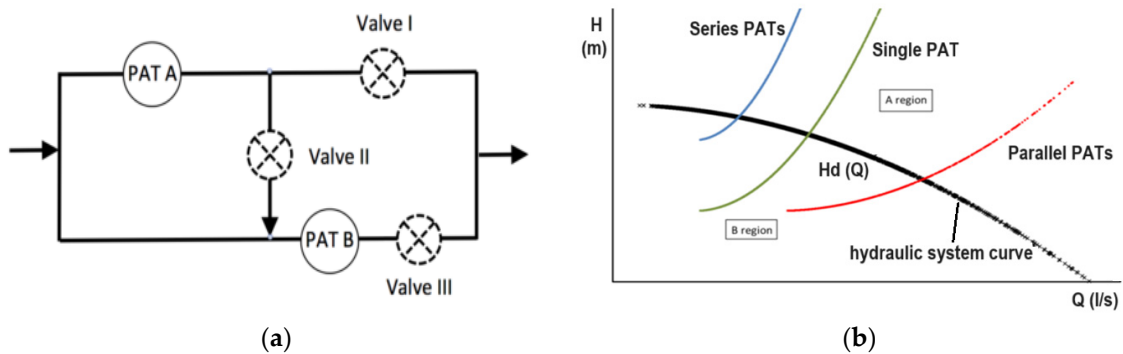


Figure 5. Scheme for single–serial–parallel (SSP) PAT mode (a), characteristic curves for SSP modes (b).

Various PAT configurations for power generation can be applied, as depicted in Figure 4, offering flexibility in implementing this technology.

The primary objective in water distribution networks is to control water losses, as this is the most important means of conserving energy and water resources. This need is of financial importance to water utilities globally and results in significant savings across the spectrum of water-related processes that include extraction, treatment, transport, and distribution. In water supply systems (WSSs), hydraulic energy resources are sometimes abundant. This inherent characteristic makes water pipelines potential sources of renewable energy. Notably, discharge nodes exhibit constant daily variations in flow rates and heads. Consequently, accurate knowledge of energy availability is critical in predicting and delineating the economic benefits of using less energy for power generation.

Control valves (CVs) are strategically positioned within water networks to separate regions of significant topographic elevation differences or reduce the remaining flow head at the end of pipelines. On the other hand, pressure-reducing valves (PRVs) are used to relieve excessive pressure in the network. However, converting excess pressure into electrical energy through pump-as-turbine systems (PAT) encounters certain limitations. The main difficulty in implementing PATs is the constant fluctuation of hydraulic conditions, characterized by varying flow rates and pressures depending on demand.

The problems with energy recovery in water networks can be solved by utilizing a unique planning technique called variable operating strategy (VOS). PATs are made useful

as energy generators in the water sector by VOS, which takes into account the temporal variations in flow rates and pressures. Hydraulic regulation (HR) and electric regulation (ER) can both benefit from the effective application of VOS to account for the fluctuating operating conditions brought on by daily water demands. It is crucial to integrate a control system for PATs in order to handle the fluctuating operating conditions brought on by daily water demand. Figure 4 illustrates the various PAT operating states: a) In hydraulic control mode (HR), the PAT installation scheme consists of two branches: a control valve and a PAT are connected in series in the first branch, which is the discharge/production branch; a regulating valve is installed in the second branch, which is the bypass (Figure 4a). When the head is available in HR mode— H_d is greater than the head that the machine supplies, H_t (points above the PAT characteristic—Figure 4b)—the excess pressure is released by the series-connected valve (Valve A).

On the other hand, if Q_d exceeds the available head (indicated by points below the PAT characteristic in Figure 4b), then a head higher than what is available is produced by the PAT. In such cases, Valve B opens up to lower the discharge from Q_d to Q_t within the PAT.

To avoid exceeding the available head, the PAT is equipped with a bypass valve. When operating in ER mode, the generator's speed adjusts to correspond with both flow rate and head at any given moment. Meanwhile, regardless of mode (HER), desired results are achieved by selecting an appropriate combination of valve regulation and machine rotational operating speed [34–37]. A variable operating strategy (VOS) employed within water distribution systems can optimize performance for both HR and ER modes via idealizing PAT selection. As far as mathematical considerations go, NR mode delivery occurs when points align on characteristic curve-to-network flow rates (as seen in Equation (4)):

$$H_t = H_t(Q_d) \quad (4)$$

where H_t is the net head delivered by the PAT (m) and Q_d is the available discharge (m^3/s).

In no regulation (NR) mode, three working regions can be defined as follows:

- Region 1— $Q_i < Q_{t,min}$: $Energy = 0$;
- Region 2— $Q_i > Q_{t,max}$ or $Q_{t,min} < Q_i < Q_{t,max}$ and $H_t > H_i$: $Energy = 0$;
- Region 3— $Q_{t,min} < Q_i < Q_{t,max}$ and $H_t < H_i$: $E = P(Q_i)\Delta t_i$.

where Q_i, H_i are the flow and the available head in the instant i ; Q_t, H_t are the turbine flow and the net head delivered by the PAT; P is the power; and Δt is the operation period. “min” and “max” are the operating extreme values of the PAT.

In HR mode, the rotational speed of the PAT is fixed, and Valves (A) and (B) control the flow through the machine (Equation (5)):

$$\begin{cases} H_d = H_t(Q_t) + H_{valve} \\ Q_d = Q_t + Q_{bypass} \\ H_{valve} > 0, Q_{bypass} = 0 \text{ if } H_t(Q_t) < H_d \\ H_{valve} = 0, Q_{bypass} > 0 \text{ if } H_t(Q_d) > H_d \end{cases} \quad (5)$$

where H_d, H_t are the available and the PAT head (m); H_{valve} is the head delivered by the valve (m); Q_t, Q_d are the turbine discharge (m^3/s) and the available discharge (m^3/s); Q_{bypass} is the bypass discharge (m^3/s).

In HR mode, four working regions can be defined:

- Region 1— $Q_i < Q_{t,min}$ or $H_i < H_{t,min}$: $Energy = 0$;
- Region 2— $Q_{t,min} < Q_i < Q_{t,max}$ and $H_i > H_t(Q_i)$: $Energy = P(Q_i)\Delta t_i$;
- Region 3— $Q_{t,min} < Q_i < Q_{t,max}$ and $H_{t,min} < H_i < H_{t,max}$: $Energy = P(Q_t(H_i))\Delta t_i$;
- Region 4— $Q_i > Q_{t,max}$ and $H_i > H_{t,max}$: $Energy = P(Q_{t,max})\Delta t_i$.

In HER mode, the HR and the ER modes are coupled to improve the performance of the PAT (Equation (6)):

$$\left\{ \begin{array}{l} H_d = H_t(Q_t, N_t) + H_{valve} \\ Q_d = Q_t(N_t) + Q_{bypass} \\ H_{valve} > 0, Q_{bypass} = 0 \text{ if } H_t(Q_t, N_t) < H_d \\ H_{valve} = 0, Q_{bypass} > 0 \text{ if } H_t(Q_d, N_t) > H_d \end{array} \right. \quad (6)$$

In HER mode, Valves (A) and (B) work together with the rotational speed regulation, allowing for better control of flow and head to maximize the energy production. Four working regions can be defined as follows:

- Region 1— $Q_i < Q_{t,min}$ or $H_i < H_{t,min}$: $Energy = 0$;
- Region 2— $Q_{t,min} < Q_i < Q_{t,max}$ and $H_i > H_t(Q_i, N_t)$: $Energy = P(Q_i)\Delta t_i$;
- Region 3— $Q_{t,min}(N_t) < Q_i < Q_{t,max}(N_t)$ and $H_{t,min}(Q_t, N_t) < H_i < H_t(Q_i, N_t)$: $Energy = P(Q_t(H_i(N_t)))\Delta t_i$;
- Region 4— $Q_i > Q_{t,max}(N_t)$ and $H_i > H_{t,max}(N_t)$: $Energy = P(Q_{t,max}(N_t))\Delta t_i$.

In these modes, the optimization process aims to achieve the combined values of flow (Q) and head (H) that maximize the energy production.

In order to face the limitations of the PAT operation for small flow values, a new PAT regulation strategy can also be presented: single–serial–parallel regulation mode (SSP). In SSP mode, the installation comprises two PATs and three on/off valves [34–37] (Figure 5).

The installation scheme of the SSP mode is illustrated in Figure 5a. The SSP mode has three different working conditions that vary based on the daily demand, as depicted in Figure 5b). These conditions are as follows: (i) valve I and PAT A are on while valves II and III plus PAT B remain off, leading to a single energy-producing PAT; (ii) both valves II and III along with PATs A and B are turned on while valve I is off, resulting in series production of energy by the two PATs; (iii) both valves I and III are open with PAT A and B running parallel, resulting in double the flow compared to operating condition (i). An increased head for serial-operated turbines was observed during operation condition (ii), shown in Figure 5b, compared to a single turbine under operating state (i). Consequently, the flow rate doubled when parallel operating turbines were employed (under operating condition (iii)), also demonstrated in Figure 5b. Thus, it can be concluded that using the SSP mode is practical for recovering energy in small energy communities [34–37].

2.3. Energy Simulator

The next step is to develop simulations in the HOMER model (Figure 6), for which the site and load data requirements must first be determined. The location for the project's case study is on Madeira Island. HOMER downloads data from NASA POWER to obtain wind speeds and solar radiation data.

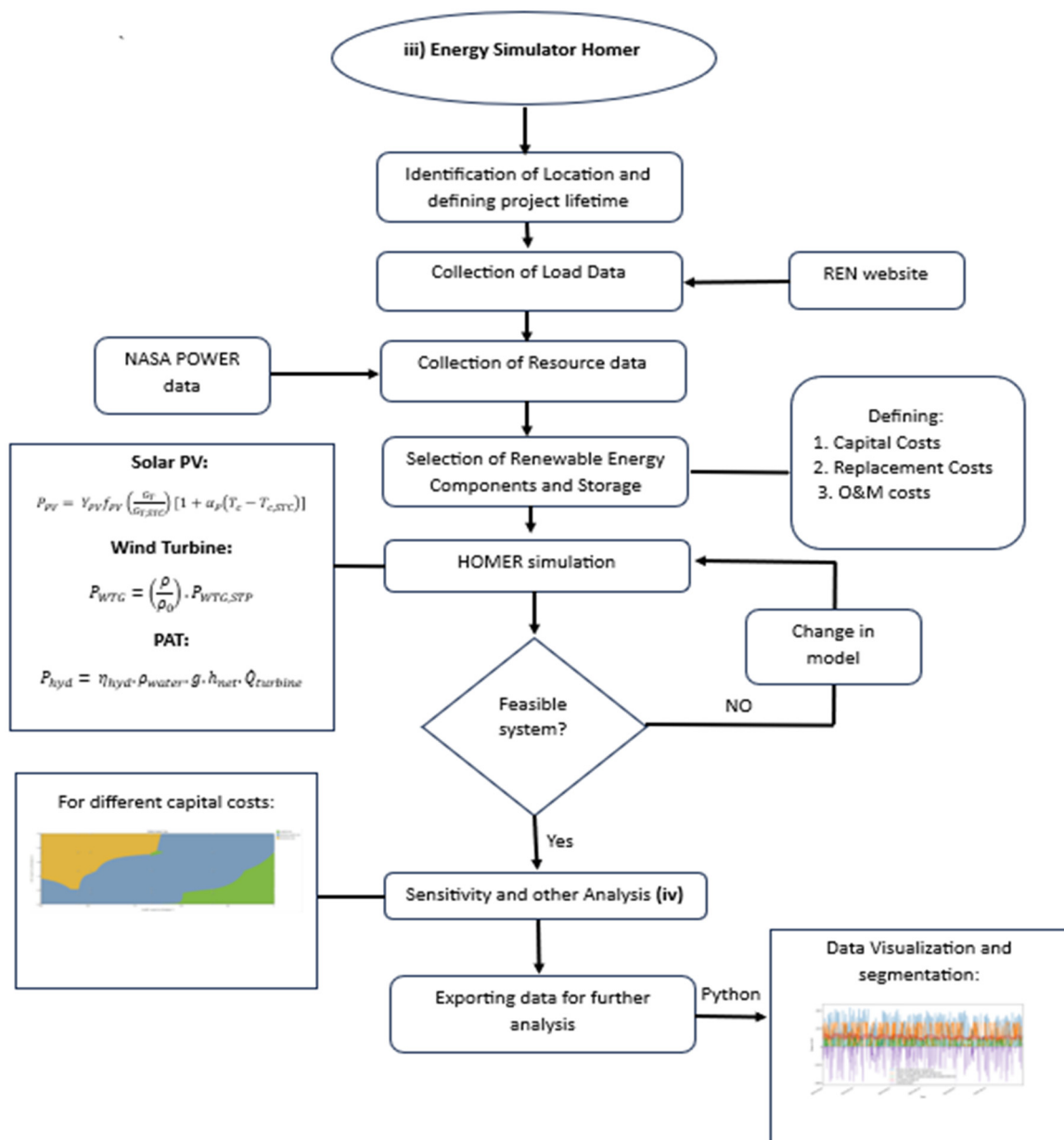


Figure 6. Energy simulator methodology.

The load for the selected project must be entered into the model. The components for the microgrid must also be selected. Renewable components include photovoltaic, wind, and hydropower (PAT). Once the renewable components have been selected, their specifications and costs must be determined. Some of the specifications are already available in the HOMER library. For the cost specifications, experts in the field can be consulted, or various platforms that provide a cost estimate for components based on their capacity can be adapted. After all the data are entered, HOMER optimizes the hybrid system based on many combinations. These results also show electrical and economic results, which can be used for further analysis.

2.4. Energy Production

Power generation from pumps as turbines (PATs) is effectively analyzed and tracked using the HOMER energy optimization model. HOMER uses a grid search algorithm and a proprietary derivative-free algorithm to determine the most cost-effective microgrid model that meets load demand. The location chosen for these simulations is the city of

Funchal in the Madeira Islands. The results of these simulations will provide valuable insight into the performance of PATs in power generation, especially when combined with hydropower.

Specific data inputs are required to perform these simulations, including load requirements, capital and operating costs, replacement costs for all energy systems to be installed, and the availability of resources such as solar, wind, hydro, and biomass at the project site. The software obtains solar, wind, and temperature data from NASA's Prediction of Worldwide Energy Resource database. To evaluate hydropower production with PATs, energy components such as solar arrays, wind turbines, hydropower, and grid connections are selected for the simulations.

Considering the different water demands, the flow rates are determined. Winter flow is calculated as 0.7 times summer flow. In comparison, spring and fall flows are assumed to be 0.85 times summer flow, with the highest demand occurring in the summer. The simulation model shown in Figure 6 includes photovoltaic systems, wind turbines, the power grid, PATs (hydro turbines), a battery for storage, and an inverter to convert DC from photovoltaic systems to AC. For flows below 35 L/s, a 5 kW water turbine is used, while for flows above 35 L/s, a 10 kW water turbine is used. The model specifies these flow rates, with a nominal flow of 35 L/s for the 5 kW water turbine and 70 L/s for the 10 kW water turbine. The efficiency of the water turbines is set at 80% for both. The simulations are performed over a project life of 25 years, considering an inflation rate of 2% and a discount rate.

To get as close as possible to real-time consumption patterns, hourly electricity consumption data for Portugal were taken from an open-source database from the website REN [42]. Then, the data adjustment was defined to represent the energy consumption at a smaller municipality level. The load data used in the simulations from HOMER show a peak electricity demand of 9.94 kW and an average daily energy consumption of 160.44 kWh. Over the year, the average electricity consumption is 6.68 kW. It is noteworthy that the highest monthly peak load occurs in January. A visual representation of the load distribution in each month can be found in Figure 7, which shows the load box plot for each month.



Figure 7. Box plot of load demand considered for the simulations.

Solar PV uses solar radiation to generate electricity. The use of solar PV renewable energy systems has been growing rapidly in recent years. The calculation of electricity generated by solar PV in the model is calculated as follows:

$$P_{PV} = Y_{PV} f_{PV} \left(\frac{G_T}{G_{T,STC}} \right) [1 + \alpha_P (T_c - T_{c,STC})] \quad (7)$$

where

Y_{PV} = power output during standard test conditions in kW.

f_{PV} = derating factor of solar PV.

G_T = incident solar irradiance in kW/m².

$G_{T,STC}$ = incident solar irradiance at Standard test conditions, which is 1 kW/m².

α_P = temperature co-efficient of power.

T_c = cell temperature of solar PV in °C.

$T_{c,STC}$ = cell temperature under standard test conditions, which is 25 °C.

Another renewable energy system growing in today's market is wind energy. Many innovative wind turbine models are on the rise to harness wind energy on both large and small scales. The wind turbine considered for the case study simulation is a generic 3 kW wind turbine predefined by the model. It first calculates the wind speed at hub height using the following equation:

$$U_{hub} = U_{anem} \cdot \frac{\ln\left(\frac{Z_{hub}}{Z_0}\right)}{\ln\left(\frac{Z_{anem}}{Z_0}\right)} \quad (8)$$

where

U_{hub} = wind speed at the hub height of the wind turbine in m/s.

U_{anem} = wind speed at the anemometer height in m/s.

Z_{hub} = hub height of the wind turbine in m.

Z_0 = the surface roughness length in m.

Z_{anem} = anemometer height in m.

After calculating the wind speed at hub height, the model considers the wind turbine's power curve to calculate the power generated by the wind turbine under standard temperature and pressure conditions. To obtain the power generated under real conditions, the model uses the following equation:

$$P_{WTG} = \left(\frac{\rho}{\rho_0}\right) \cdot P_{WTG,STP} \quad (9)$$

where

P_{WTG} = output power of wind turbine in kW.

$P_{WTG,STP}$ = output power of wind turbine at standard temperature and pressure in kW.

ρ = actual air density in kg/m³.

ρ_0 = air density at STP, which is 1.225 kg/m³.

Hydropower is one of the oldest techniques of energy generation. For this research, a 5 kW hydro turbine was chosen for lower flow rates and a 10 kW hydro turbine for higher flow rates. These water turbines represent the PATs that can be installed at the locations of the pressure-reducing valves. The calculation for the water turbine, which is a PAT, is given as follows:

$$P_{hyd} = \eta_{hyd} \cdot \rho_{water} \cdot g \cdot h_{net} \cdot \dot{Q}_{turbine} \quad (10)$$

where

P_{hyd} = hydro turbine power output in kW.

η_{hyd} = efficiency of hydro turbine in %.

ρ_{water} = water density, which is 1000 kg/m³.

g = acceleration due to gravity 9.81 m/s².

h_{net} = effective head in m.

$\dot{Q}_{turbine}$ = hydro turbine flow rate in m³/s.

The simulation for all selected valves had the same load and the same renewable energy microgrid system (Figure 8) to better understand the LCOE, NPC, and other economic parameters.

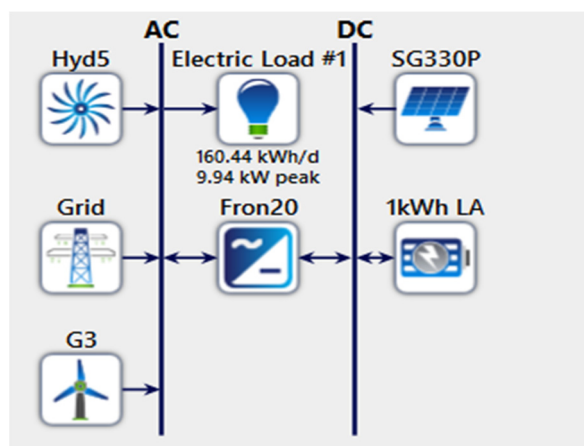


Figure 8. Microgrid system for all simulations of PATs and other components.

2.5. Methodology for the Analysis of Results

The HOMER model acts as an optimizer for renewable energy systems, offering potential and feasible solutions. It selects the case with the lowest net present cost (NPBC) for a comprehensive analysis. It also performs detailed calculations to evaluate the benefits of incorporating pumps as turbines (PATs) into the microgrid system. The Electrical Analysis component of HOMER provides valuable insight into the role of PATs in power generation. It allows for the power generation of all power systems to be considered. It provides insight into each system’s individual contribution and the lowest electricity cost (LCOE). It also provides insight into grid purchase and recovery values, facilitating analysis of the interplay between each energy component’s power generation and its impact on costs and benefits.

Sensitivity analysis is proving to be a valuable tool for understanding the importance and role of a power system within the microgrid system. Manipulating parameters such as the capital cost multiplier or the costs associated with a power system identifies a microgrid system with the lowest NPC, providing important insights for decision-making and optimization (Figure 9).

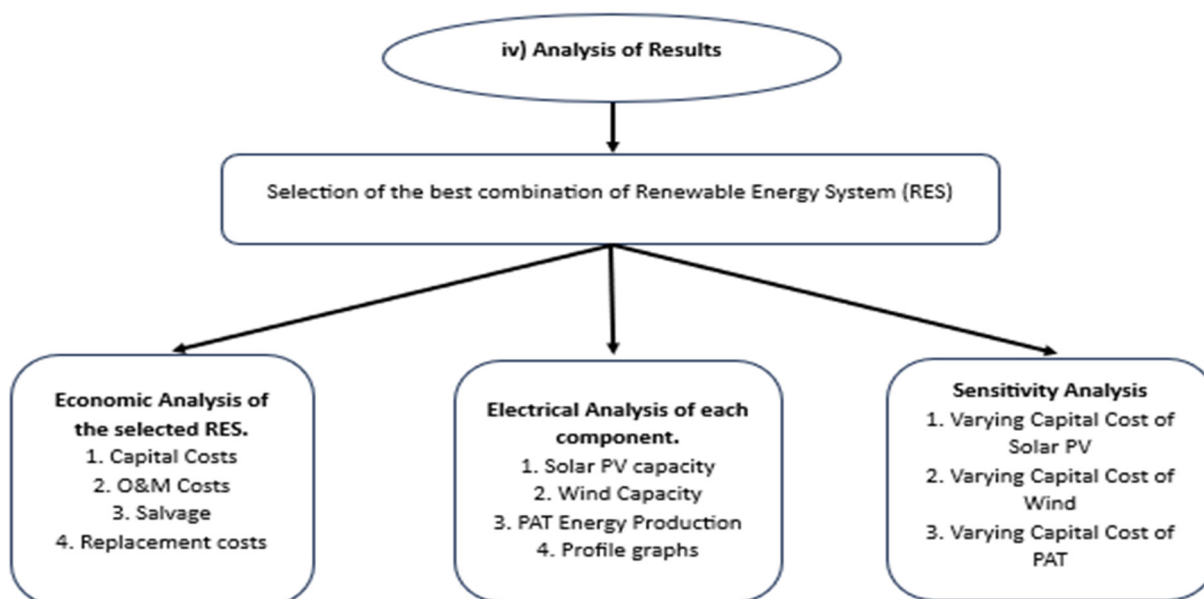


Figure 9. Procedure for analysis of results.

The net present cost of the system is all costs of the project incurred during its life and reported at present value. This includes O&M costs, capital costs, and replacement costs. These costs are calculated by HOMER using the discount factor to obtain discounted cash flows.

$$NPC = \text{Capital Cost} + \text{Replacement Cost} + \text{O\&M Cost} + \text{grid purchase cost} - \text{Salvage} \quad (11)$$

Levelized cost of energy production (LCOE) is the ratio of the annual average cost of the project and the total electricity load served. LCOE is an essential economic factor in considering the attraction towards a project. This is calculated using the following equation:

$$LCOE = \frac{C_{ann,tot}}{E_{served}} \quad (12)$$

where

$C_{ann,tot}$ = total annualized cost of the system in EUR/year.

E_{served} = total electrical energy served in kWh/year.

The model uses the nominal interest and inflation rates as inputs to calculate the real discount rate. This is used to calculate the discount factor, which is used to calculate the annualized cost. The calculation for the discount rate is as follows:

$$i = \frac{i' - f}{1 + f} \quad (13)$$

where

i = real discount rate.

i' = nominal discount rate.

F = expected inflation rate.

According to the simulation in this research, $i' = 8\%$ and $f = 2\%$, and i can easily be calculated by

$$i = \frac{0.08 - 0.02}{1 + 0.02} = 0.059 \quad (14)$$

The discount factor is a ratio that can be used to obtain the present value of costs in any year of the project. This factor is used to express, at present value, the savings that will be realized over the project's life. The discount factor can be calculated using the following equation:

$$f_d = \frac{1}{(1 + i)^N} \quad (15)$$

where

f_d = discount factor.

i = real discount rate.

N = number of years.

The discount factor in all simulations in this research for the 25th year can be calculated as follows:

$$f_d = \frac{1}{(1 + 0.059)^{25}} = 0.238$$

The renewable energy investment is the NPC of all renewable energy systems installed in the microgrid system. This value is calculated by subtracting the grid purchase cost from the total useful life. This value indicates the actual investment made in renewable energy.

$$NPC \text{ of Renewables} = NPC \text{ of Project} - \text{grid purchases} \quad (16)$$

The main benefit of installing renewable energy systems is the consumption of locally generated energy. The savings can be determined by calculating the total energy produced by all renewable energy and calculating the bills that would have to be paid if the same energy was consumed from the grid. This value shows the monetary savings from consuming energy without paying bills. The value is calculated by multiplying the grid purchase cost, set at 0.258 kW/h, by the energy generated by the renewable energy sources during the project period. The meaning of this value is derived from calculating the value of net present cost savings.

$$\text{Savings at } 0.258 \frac{\text{€}}{\text{kWh}} \text{ grid price} = \left\{ \text{Solar PV} \left(\frac{\text{kWh}}{\text{yr}} \right) + \text{Hydro} \left(\frac{\text{kWh}}{\text{yr}} \right) + \text{Wind} \left(\frac{\text{kWh}}{\text{yr}} \right) \right\} \times 0.258 \frac{\text{€}}{\text{kWh}} \times 25 \text{ yr} \quad (17)$$

Net present savings is an external calculation created from the software results to highlight the microgrid's economic advantage and the contribution of PATs. This value is the cost savings over the project's life, expressed as a present value. This value is calculated by multiplying the cost savings over the project's life by the discount factor (fd). This value gives an idea of the profits that can be calculated by deducting the savings, i.e., the revenues from the renewable energy NPC.

$$\text{Net Present Savings} = 0.238 * \text{Savings at } 0.258 \frac{\text{€}}{\text{kWh}} \text{ grid price} \quad (18)$$

Net present value (NPV) is the difference between the revenue or savings generated by the project discounted to the current year of consideration. A positive NPV means that the project is attractive. When the project is initiated, the NPV can be calculated as follows:

$$\text{NPV} = \text{NPC} - \text{Net Present Savings} \quad (19)$$

Return on investment (ROI) is an essential factor when considering the investment in a project. It is calculated by dividing the profits by the cost of the project. ROI for the simulation results is calculated externally in this research by calculating the net profit, which is the difference between the renewable energy investment and the net savings. This value is further divided by the renewable energy investment as shown in the equation:

$$\text{ROI} = \frac{\text{Net Present Cost Savings (€)} - \text{NPC of Renewables (€)}}{\text{NPC of Renewables (€)}} \quad (20)$$

The costs are entered into the model to calculate the lowest-cost microgrid system. These costs are used to calculate net present costs (NPCs), LCOE, CAPEX, and OPEX.

The cost of photovoltaic systems has been decreasing over the years, and the cost of simulating photovoltaic systems includes all equipment, including wiring and labor for installation. The cost of the wind turbine, battery, and inverter are predefined in the software package HOMER. The grid electricity price is set at 0.258 EUR/kWh, and the grid feedback price at 0.030 EUR/kWh. The costs of the different components used are listed in Table 1.

Table 1. Costs of various components used in the simulation.

Component	Capital Cost	Replacement Cost	O&M Cost
Solar PV (SG330P)	1000 EUR/kW	1000 EUR/kW	30 EUR/year
Wind turbine (G3)	18,000 EUR/unit	18,000 EUR/unit	180 EUR/year
Battery 1 kWh lead acid	300 EUR/unit	300 EUR/unit	10 EUR/year
Inverter	2500 EUR/unit	2500 EUR/unit	20 EUR/year
Hydro turbine (5 kW)	2500 EUR/unit	1250 EUR/unit	500 EUR/year
Hydro turbine (10 kW)	5000 EUR/unit	2500 EUR/unit	800 EUR/year

3. Results and Discussion

3.1. Brief system Definition

The investigation of energy recovery methods in this study was carried out using a specific framework aimed at controlling water losses. This study was carried out in the municipality of Funchal (CMF), in a pilot area where a comprehensive study on the control of water losses had previously been developed (Figure 10).

The municipality's water supply system benefits from the natural topography and relies on gravity reservoirs that receive water from the Águas e Resíduos da Madeira (ARM) supply system and neighboring municipalities. Given the predominantly residential nature of the region and the high population density, water consumption is remarkably high, requiring an efficient and well-managed system.

However, a thorough analysis of the components of water losses based on data provided by the Camara Municipal do Funchal (CMF) revealed the urgent need to implement a strategy focused on reducing actual water losses, representing 90% of total losses in the pilot zone. Furthermore, the total water losses comprised over 60% of the entire amount discharged into the system. This presents a notable financial obstacle to the water utility and poses an ecological danger to its ecosystem. These circumstances emphasize that there is a pressing need to diminish water losses below 20%, as dictated by national protocols.

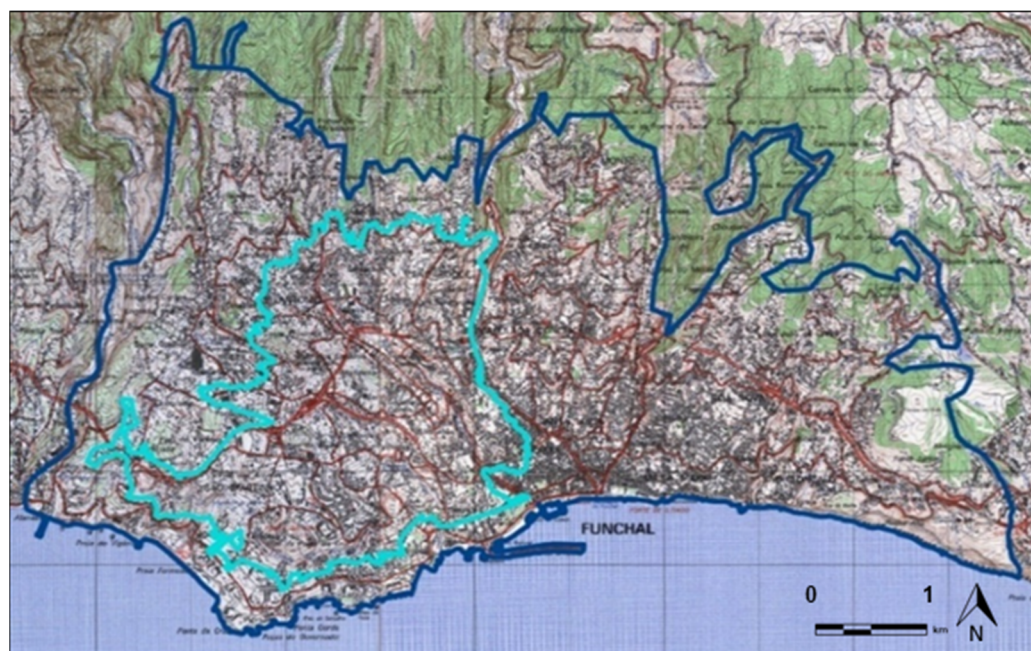


Figure 10. Funchal municipality (dark blue) and pilot zone (light blue).

The overarching strategy was developed based on the Institute for Water and Waste Regulation (IRAR) Leakage Control Protocol to address and correct the situation described above. This protocol includes several essential steps, including the following:

- Establishment of district metered areas (DMAs): This means creating defined zones within the distribution system to facilitate the metering and regulation of pressure levels and flow rates in each area. In the first phase, the primary areas of influence are delineated.
- Effective pressure management: This step focuses on properly regulating pressure to avoid excessive water loss and ensure adequate water supply to consumers.
- Active damage control: In this phase, measures are taken to detect and repair leaks in the system in good time.

The following subsections provide a comprehensive overview of the current situation and elaborate on the specific procedures used to address this issue.

3.2. Hydraulic Simulations

3.2.1. Hydraulic Scenarios

To gain insight into the causes of water loss and determine the most effective loss control strategy, a basic hydraulic model was created using EPANET software. This step proved critical in conducting a diagnostic assessment of current circumstances. It helped inform decision-making regarding establishing district metering areas and intermediate pressure stages. These elements were the initial building blocks for creating the “New Situation” model (see Figure 11). The hydraulic simulation used the Hazen–Williams equation to compute head losses by applying distinct roughness coefficients: values of 140 for recently installed HDPE or cast iron pipelines, 130 for pre-existing HDPE or cast iron pipes, 120 for steel or PVC pipes, and, lastly, 100 was used for fiber and galvanized metal pipe material.

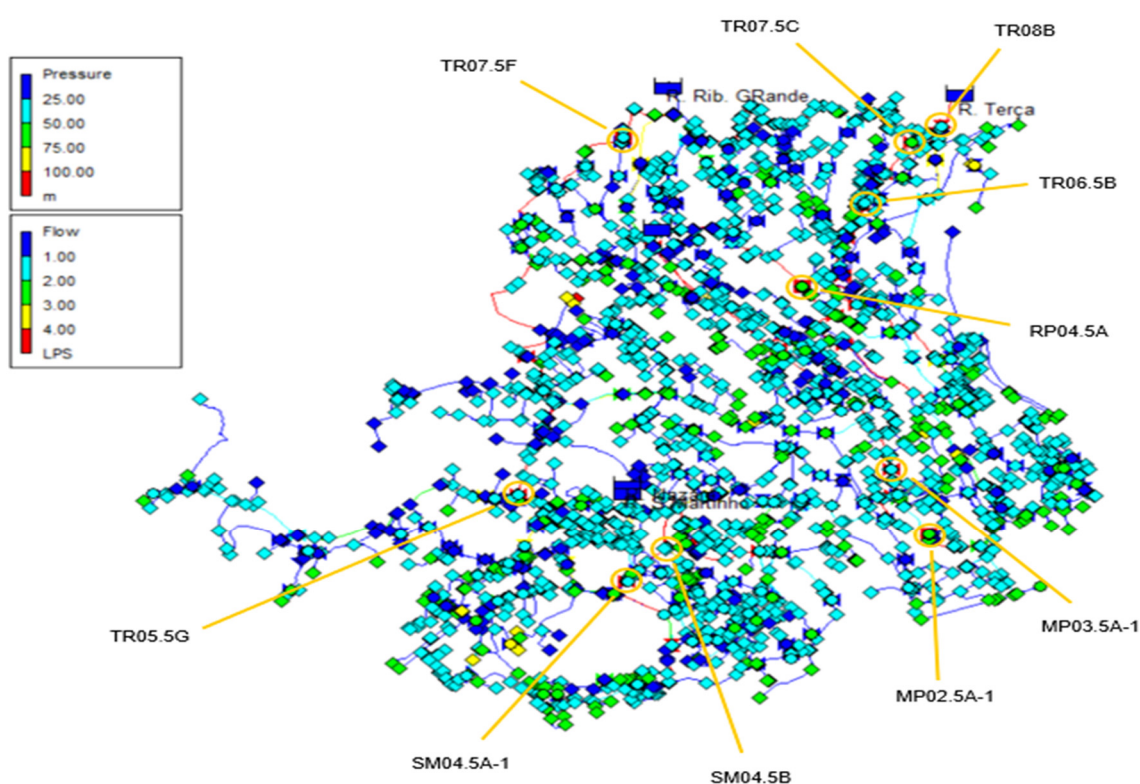


Figure 11. Selected PRV for PAT implementation.

In an initial review of the hydraulically constructed model, we found specific deficiencies in the hierarchical structure of the network. In addition, the evaluation showed that the pressure drops in the network were relatively low, which could lead to increased water pressure and consequently to the risk of fractures and leaks. This problem is visually represented in Figure 12a, where areas exceeding the legal maximum pressure of 60 m of water column (m w.c.) are highlighted in yellow. Consumption requirements in the intersections are shown in Figure 12b.

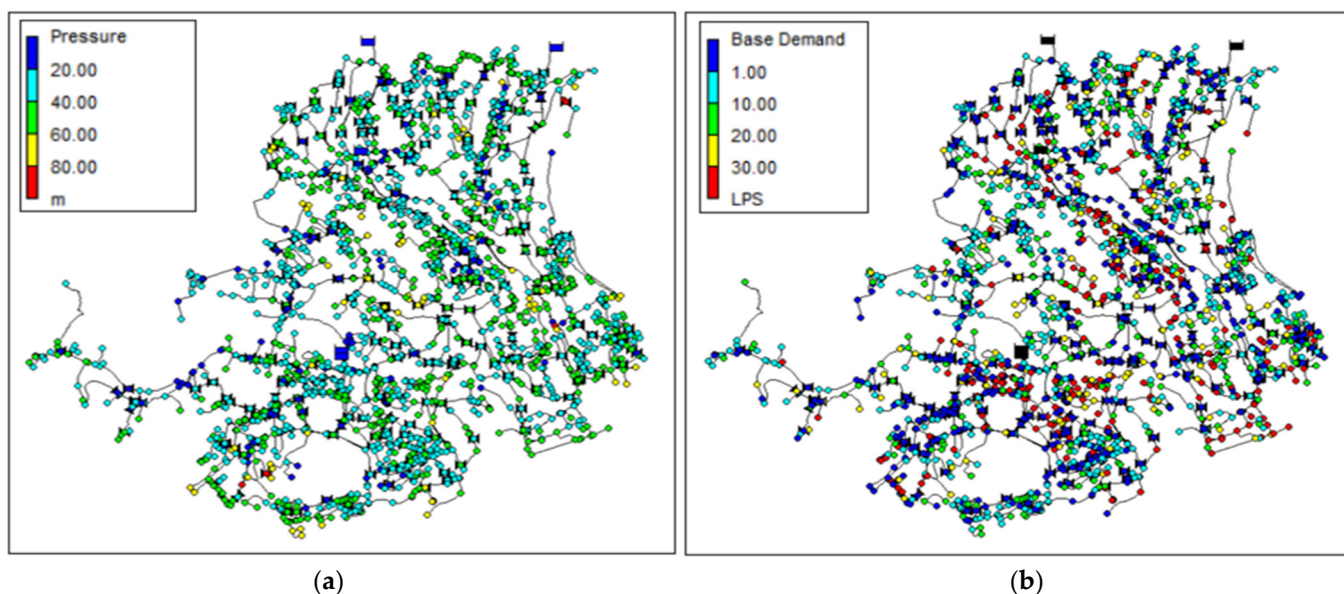


Figure 12. EPANET model—pressure levels in network junctions (a) and consumption demand on network junctions (b).

The EPANET model developed has proven invaluable in providing crucial insights into the pressure dynamics of the water network. On average, the pressure is about 53 m w.c. and occasionally rises to about 100 m w.c.

The developed model corresponds to the current situation and includes all previously defined mitigation measures, such as implementing newly installed PRVs and establishing new DMAs. Figure 13 shows the EPANET model, which shows the network nodes' pressure levels and consumption demand.

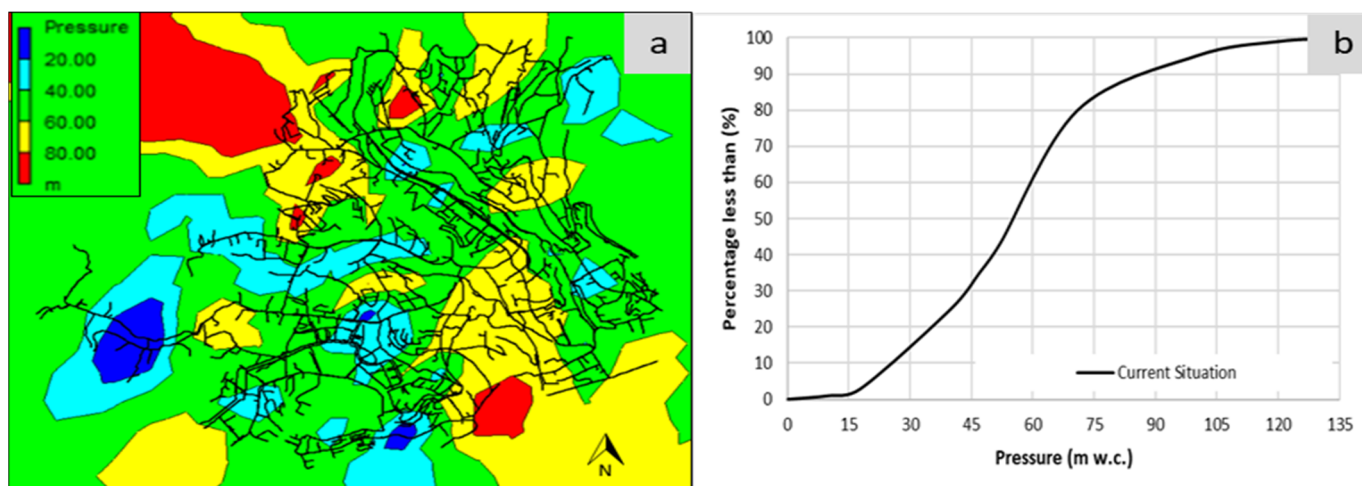


Figure 13. The current situation is spatial pressure distribution at 13:00 (a) and a percentage of less than a particular pressure value (b).

The hydraulic simulator model was significantly improved as part of the new improved scenario. This included the creation of 30 new district metered areas (DMAs) with an average extent of 6 km each. In addition, 50 new pressure-reducing valves (PRVs) were added to the model to provide additional pressure levels. In addition, certain existing valves were adjusted, i.e., both opened and closed, and approximately 11 km of new piping was added to the network. These measures enabled a more uniform pressure distribution, resulting in lower average and maximum pressure values (Figure 14).

After simulating this revised scenario, a brief analysis of the results revealed several noteworthy findings:

- (i) The pressure values of the network decreased to an average value of about 37 m w.c., which is a decrease of 16 m w.c. compared to the previous scenario.
- (ii) Only 4% of the nodes in the network registered a minimum pressure above the legal maximum of 60 m w.c.—a significant decrease (35%) from the previous scenario. Moreover, this figure increased slightly to 5% when studied under static boundary conditions, in stark contrast to the 50% recorded in the existing scenario.
- (iii) It is particularly noteworthy that most of the network is no longer under excessive pressure, with an average reduction of about 1.6 bar compared to the current situation.

These results underscore that the excessive pressure from sectorization efforts has been significantly alleviated.

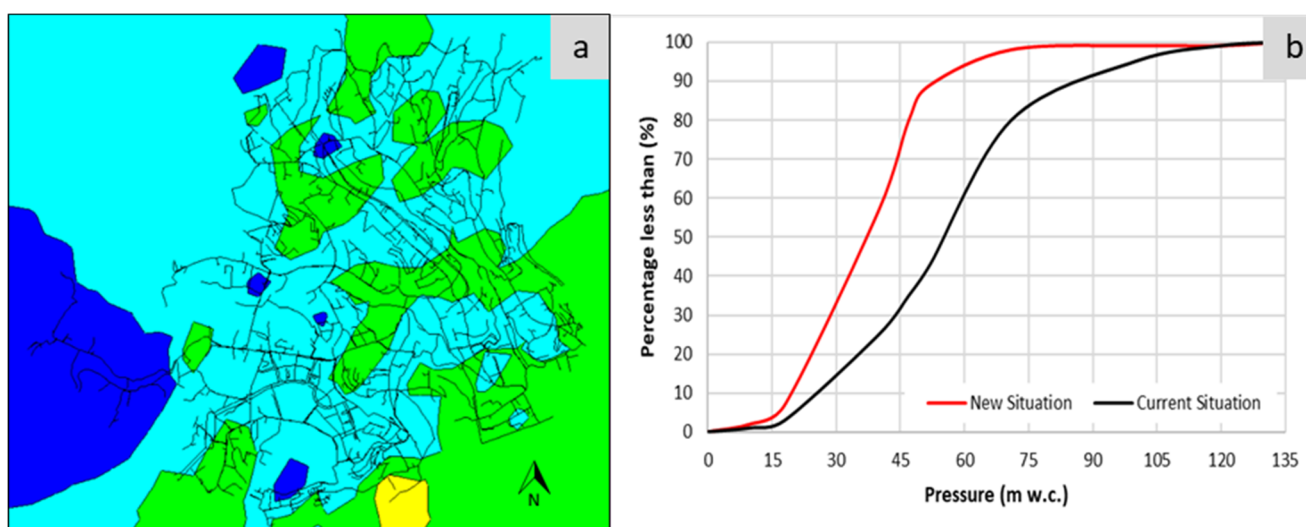


Figure 14. New situation spatial pressure distribution at 13:00 (a) and percentage of less than a particular pressure value (b).

In the new scenario, the proportion of the network exposed to high pressure decreased significantly, and pressure fluctuations decreased noticeably. To illustrate, in the current model, 40% of the network nodes were exposed to pressures above 60 m w.c. In the new model, this number increased to almost 6%.

In addition, it is essential to highlight the establishment of new district metered areas (DMAs) and the introduction of additional pressure-reducing valves (PRVs). In addition, the existing pressure-reducing valves with different pressure drops were fine-tuned, and flow meters were strategically placed in front of these valves. These measures were implemented to recalibrate the pressure in the network and exert better control over flow dynamics. Overall, these improvements reduced water losses and lowered the probability of system breaks in the distribution network.

3.2.2. PRV and PAT Characteristics

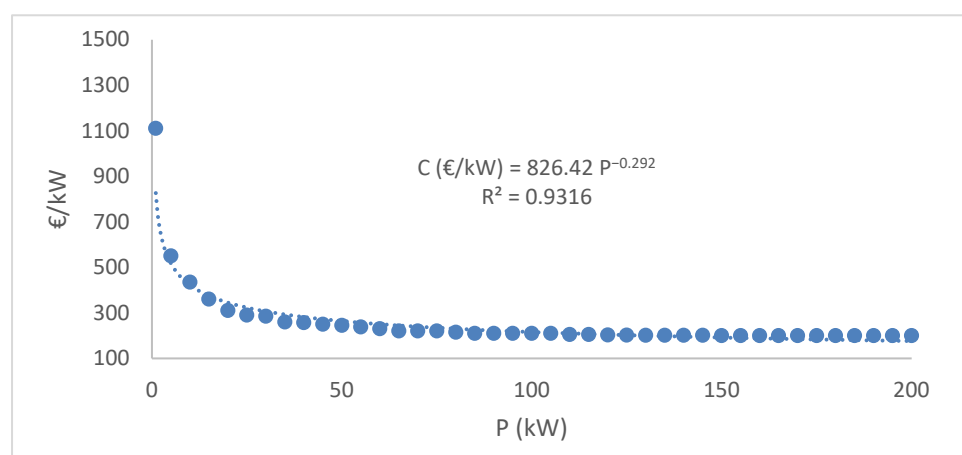
Without data on PRV prices, a correlation between valve diameter and price is assumed based on multiple valves from a particular manufacturer (Tecnilab). The estimated cost of PRVs was derived from available average market prices (Table 2). These costs are comparable to the costs of PATs. Recent studies [43] show a cost comparison of four different PAT options: a radial pump with one, two, or three pairs of magnetic poles (pp) and a vertical multistage pump with one pair of magnetic poles. The radial pumps (the most commonly used) have similar costs and are less expensive than vertical multistage pumps. The vertical pumps are more efficient for a more extensive flow range.

Table 2. PRV price *.

DN	EUR
100	2260
300	8060
600	25,300
1260	55,838

* The PRV prices used were obtained from Tecnilab.

For the PAT application, the price for each PAT is determined based on the maximum power of each device. The price varies with the maximum power generated by each PAT: the greater the installed power, the lower the unit cost (Figure 15).

**Figure 15.** Proposed PAT unit cost vs. power based on several machines.

Despite the availability of numerous potential sites for energy recovery based on the location of PRVs, only ten pressure-reducing valves (PRVs) were selected for pump-as-turbine (PAT) installation (Table 3). This selection was deemed sufficient to gather the necessary data to evaluate the energy recovery potential of the network in small communities with local power generation. The selection process included a preliminary assessment of each PRV's suitability for PAT implementation. Specifically, the pressure drop provided for each PRV was multiplied by its flow rate. Then, the 10 PRVs with the highest values, represented as QH (flow rate multiplied by pressure drop), were selected for subsequent in-depth analysis.

Table 3. PRVs selected for PAT implementation.

PRV (-)	D Pipe (mm)	D Valve (mm)	Q (L/s)	V (m/s)	Upstream Pressure (m)	Downstream Pressure (m)	Head Drop (m)	QH (-)
MP-03.5A-1	250FF	150	32.20	1.82	44.75	23.71	21.04	6.64
MP-02.5A-1	250FF	150	20.66	1.17	52.27	22.35	29.92	6.06
SM04.5A-1	200FF	150	25.68	1.45	40.1	17.80	22.3	5.61
SM04.5B	200FF	200	43.12	1.37	53.36	29.80	23.56	9.96
RP04.5A	250FC	150	24.65	1.39	55.66	31.10	24.56	5.93
TR08B	500FF	300	152.41	2.16	44.26	25.55	18.71	27.95
TR07.5C	200FF	150	24.12	1.36	49.7	25.25	24.45	5.78
TR06.5B	200FF	150	22.47	1.27	48.6	24.30	24.3	5.35
TR05.5G	200FF	150	26.89	1.52	47.37	24.28	23.09	6.08
TR07.5F	400FF	300	82.28	1.16	44.15	21.60	22.55	18.18

Some options have been defined. The results of the optimal fixed ER energy for each PRV site, along with the respective optimal PAT selection and rotation speed, are shown in Table 4. Note that the NR mode does not correspond to each PAT's optimal energy recovery scenario. Table 4 shows the selected PAT type, optimal fixed rotation speed, and energy production.

Table 4. Type of PAT for optimal fixed rotation speed and energy production.

PRV	PAT	Speed (rpm)	E _{max} (MWh)
MP-03.5A-1	65–250	1120	125.7
MP-02.5A-1	65–250	770	34.3
SM04.5A-1	65–250	1170	142.1
SM04.5B	65–250	1370	328.6
RP04.5A	65–250	1020	87.4
TR08B	100–200	1310	1005
TR07.5C	65–250	1070	111.7
TR06.5B	65–250	1020	87.9
TR05.5G	65–250	1170	149.9
TR07.5F	80–200	1470	686.7

A careful examination of Table 4 reveals a discernible correlation between the power generated and the pump as turbine (PAT) speed. This relationship is likely a result of the typically higher flow rates in pressure-reducing valves (PRVs) with greater energy output, which require higher speeds for the PATs to achieve their optimum energy recovery capability.

However, an exception to this trend is PAT 100–200 in PRV TR08B, which produces three times the power compared to PAT 65–250 in PRV SM04.5B, although it has a lower speed. This discrepancy can be attributed to the broader characteristic curve of PAT 100–200 at the rated speed, which affects the optimum speed.

Another crucial aspect is the relationship between the maximum energy generated and the appropriate PAT selection for each scenario. While PAT 100–200 proves optimal for PRV TR08B, PRV MP02.5A-1 provides the highest energy yield when paired with PAT 65–200. This phenomenon underscores that higher energy production is often associated with higher discharge rates and head, which typically requires larger turbomachinery to maximize energy recovery potential.

3.3. HOMER Simulation

The simulations conducted as part of HOMER provide valuable insight into the economics and power generation within the microgrid. These simulations illuminate the central role that pumps as turbines (PATs) play in the economic dynamics of the project. The methodology includes the definition of various economic terms. It presents results demonstrating the cost benefits of incorporating PATs into microgrids.

The optimization process of the software revolves around meeting electricity demand through the judicious use of energy systems and available resources. The simulations consider different flow values with an underlying constraint on grid purchases that aims to limit CO₂ emissions to 10,000 kg/year. The results of these simulations highlight the importance of hydropower through PATs in reducing costs and increasing profits in a relatively short time frame.

It is worth noting that the TR08B valve has the highest net present value (NPV) and economic benefit, primarily due to a higher flow rate. Conversely, the lowest NPV was observed for valve TR06.5B. In addition, hydropower, represented by PATs, has the lowest LCOE compared to all other energy systems considered in all scenarios studied. Table 5 summarizes the economic benefits using metrics such as return on investment (ROI) and

net present value to consolidate the economic aspects. Table 6 summarizes the technical results of all scenarios to provide a comprehensive overview.

Table 5. Brief simulation results after optimization with HOMER for different valves and a lifetime of 25 Years.

Valve	NPC of the Project (EUR)	LCOE of the Project (EUR/kWh)	Investment in Renewables (EUR)	Savings at 0.258 EUR/kWh Grid Price (EUR)	Net Present Savings (EUR)	ROI	NPV (EUR)
MP-03.5A-1	94,006.96	0.1157	47,461.05	313,869.90	74,701.04	0.574	27,239.99
MP-02.5A-1	100,356.40	0.1227	49,507.50	308,155.20	73,340.94	0.481	23,833.44
SM04.5A-1	108,988.70	0.1172	61,429.77	365,179.65	86,912.76	0.415	25,482.99
SM04.5B	52,401.24	0.0651	21,552.70	340,512.90	81,042.07	2.76	59,489.37
RP04.5A	101,947.40	0.1233	51,303.12	312,508.95	74,377.13	0.45	23,074.01
TR08B	-4903.11	-0.00342	15,342.01	714,414.90	174,933.86	10.083	159,591.85
TR07.5C	104,437.60	0.1214	54,795.61	329,782.05	78,488.13	0.432	23,692.52
TR06.5B	114,661.00	0.1259	66,552.13	355,891.65	84,702.21	0.273	18,150.08
TR05.5G	100,045.10	0.1225	49,081.53	307,426.35	73,167.47	0.491	24,085.94
TR07.5F	11,755.49	0.01186	15,342.01	487,878	116,114.96	6.568	104,359.47

Table 6. Contribution of all energy systems in the microgrid and electrical specifications.

Valve	Q (l/s)	H (m)	QH	Solar PV SG330 P (kWh/yr)	Wind Turbine G3 (kWh/yr)	Hydro Output (kWh/yr)	Grid Purchase (kWh/yr)	LCOE of PAT (Hydro)
MP-03.5A-1	32.20	21.04	677.5	13,800 (21.4%)	7915 (12.3%)	28,421 (44%)	14,455 (22.4%)	0.0244
MP-02.5A-1	20.66	29.92	618.1	15,690 (24%)	7915 (12.1%)	25,932 (39.7%)	15,794 (24.2%)	0.0267
SM04.5A-1	25.68	22.30	572.6	25,025 (34.4%)	7915 (10.9%)	24,023 (33%)	15,812 (21.7%)	0.0289
SM04.5B	43.12	23.56	1015.9	11,066 (17.5%)	Not installed	42,618 (67.3%)	9680 (15.3%)	0.0163
RP04.5A	24.65	24.56	605.4	17,680 (26.5%)	7915 (11.8%)	25,397 (38%)	15,810 (23.7%)	0.0273
TR08B	152.41	18.71	2851.5	Not installed	Not installed	110,762 (100%)	Not purchased	0.0107
TR07.5C	24.12	24.45	589.7	20,680 (29.9%)	7915 (11.4%)	24,740 (35.8%)	15,813 (22.9%)	0.0280
TR06.5B	22.47	24.30	546.0	34,436 (42.5%)	7915 (9.76%)	22,906 (28.3%)	15,810 (19.5%)	0.030
TR05.5G	26.89	23.09	620.8	15,137 (23.3%)	7915 (12.2%)	26,047 (40.1%)	15,819 (24.4%)	0.0266
TR07.5F	82.28	22.55	1851.3	Not installed	Not installed	75,640 (98.7%)	1003 (1.31%)	0.0157

Using power generation from water distribution networks and exploring small-scale hydropower generation opportunities are new technologies that contrast with established large-scale hydropower facilities. The resulting findings relate to the economics of the proposed project. Determination of renewable resource investment, grid price savings, net savings (NPS), and net present value (NPV) was performed externally following the equations presented in the Methodology section.

Table 5 shows a consistent positive NPV for all project scenarios where PATs replace or are coupled with existing NPVs, depending on the pressure control required. This indicates that the project delivers favorable outcomes and is an enticing investment opportunity. It can be seen that an increased contribution of hydropower or an increased value of QH leads to a corresponding increase in NPV, highlighting the direct correlation between hydropower production and the NPV of the project, as visually illustrated in Figure 16.

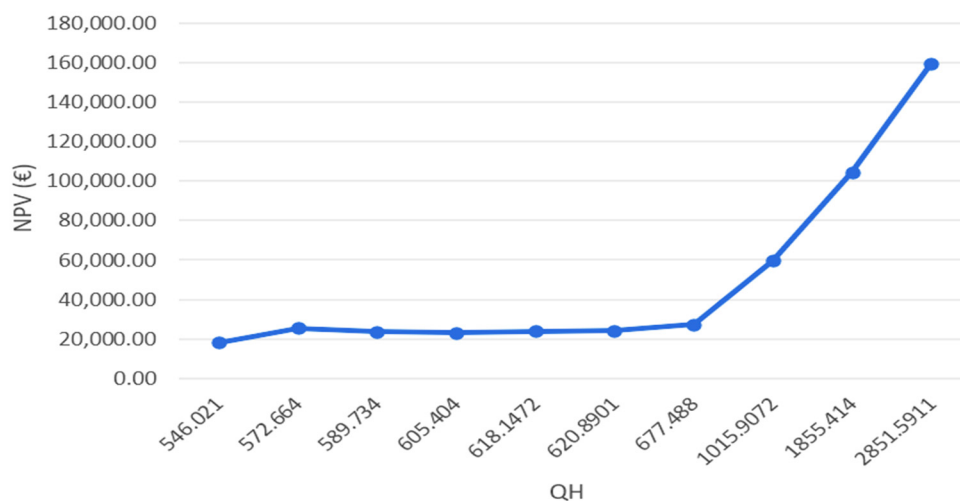


Figure 16. NPV vs. QH for all the valves replaced with PATs in the microgrid.

The most important source of savings and benefits is in avoiding the purchase of grid electricity. Solar photovoltaic (PV) systems are limited to daylight hours. At the same time, small-scale wind energy has variable power output, reducing reliability. Hydroelectric PATs can generate power throughout the day, which is consistent with the constant demand for water. Most importantly, the higher flow rates (QH) associated with PATs, such as the TR08B valve, contribute to their cost-effectiveness, as shown in the LCOE data in Table 6. These versatile PAT devices are used in various contexts, including small watercourses, water treatment plants, distribution networks, and more. The favorable LCOE profile of PATs results in significant cost benefits, especially when integrated into municipal networks with the necessary engineering considerations. This integration can lead to lower energy costs for consumers. In addition, PATs play a central role in smart cities, particularly in response to the increasing demand for electric vehicle (EV) charging infrastructure. Given the rise in summer tourism associated with high water demand, off-grid technologies using PATs offer a significant advantage in relieving the strain on the power grid associated with EV charging. Using PATs can potentially reduce the cost of electric vehicle charging, which benefits a broader consumer base.

The most important source of savings and benefits is in avoiding the purchase of grid electricity. Solar photovoltaic (PV) systems are limited to daylight hours. At the same time, small-scale wind energy has variable output, resulting in reduced reliability. Hydroelectric PATs for hydropower can generate power throughout the day, consistent with the constant demand for water. Most importantly, the higher flow rates (QH) associated with PATs, e.g., through valves such as the TR08B valve, contribute to their cost-effectiveness, as shown in the LCOE data in Table 6. These versatile PAT devices are used in various applications, including small watercourses, water treatment plants, distribution networks, and more. The favorable LCOE profile of PATs results in significant cost benefits, especially when integrated into municipal networks while addressing networks with the necessary technical requirements. This integration can lead to lower energy costs for consumers. In addition, PATs play a central role in smart cities, especially in response to the increasing demand for electric vehicle (EV) charging infrastructure. Given the increase in

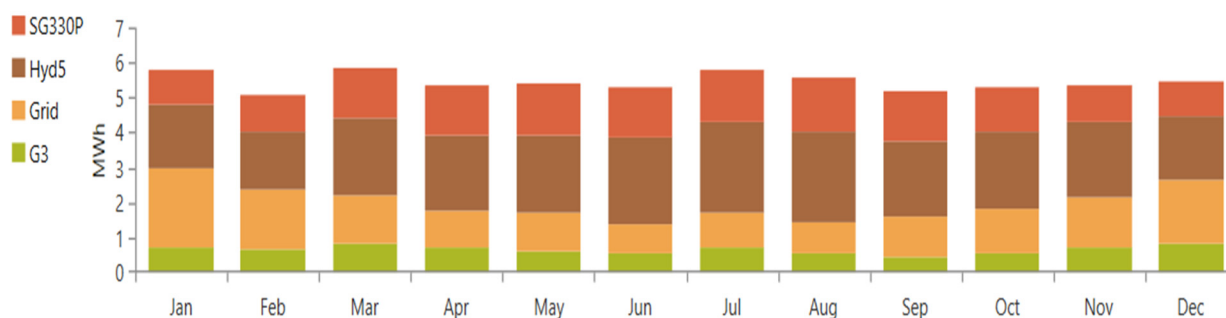
summer tourism associated with high water demand, off-grid technologies that use PATs offer a significant advantage in relieving the strain on the power grid associated with electric vehicle charging. Using PATs can potentially reduce the cost of electric vehicle charging, which benefits a broader consumer base.

- MP-02.5A-1: Illustration of the valve with the lowest flow value.
- SM04.5B: Identifies the valve with a flow value approximately equal to the average flow of all valves.
- TR08B: Designates the valve with the highest flow value.

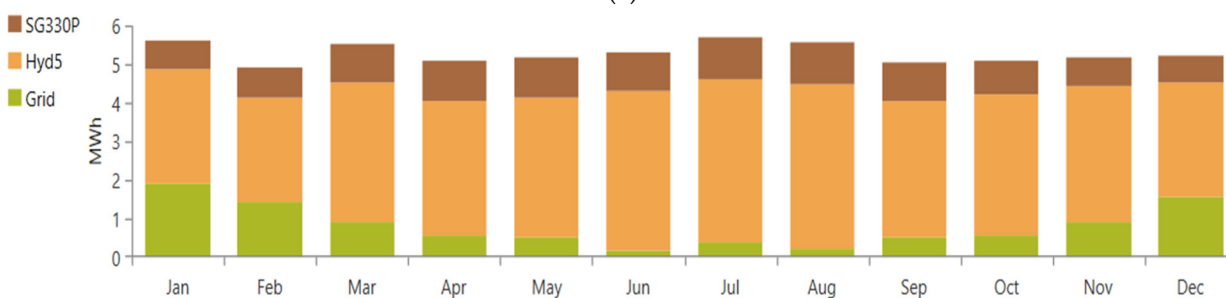
These three scenarios provide insight into how the model responds when integrating different energy systems. The main objective of the model is to optimize the microgrid system to achieve the most cost-effective configuration while ensuring that energy needs are met. This optimization strategy, known as “load tracking”, prioritizes the satisfaction of load demand. Table 7 lists the codes for each energy component. Figure 17a–c graphically illustrate the power generation required to meet the different load demands for the various microgrid configurations defined in these cases.

Table 7. Energy system code identification.

Energy System	Identification
G3	Generic 3 kW wind turbine
Hyd5	Generic 5 kW hydro turbine
SG330P	Solar PV
1kWh LA	Lead acid battery
Grid	Grid integration



(a)



(b)

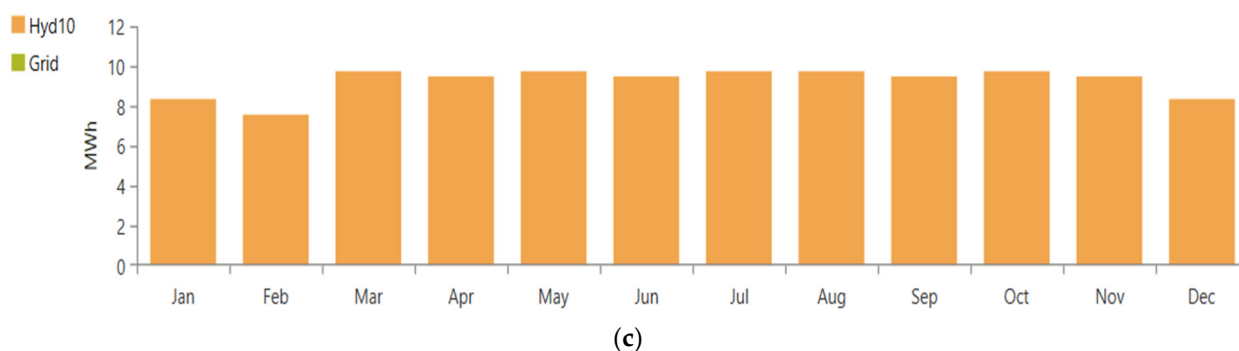
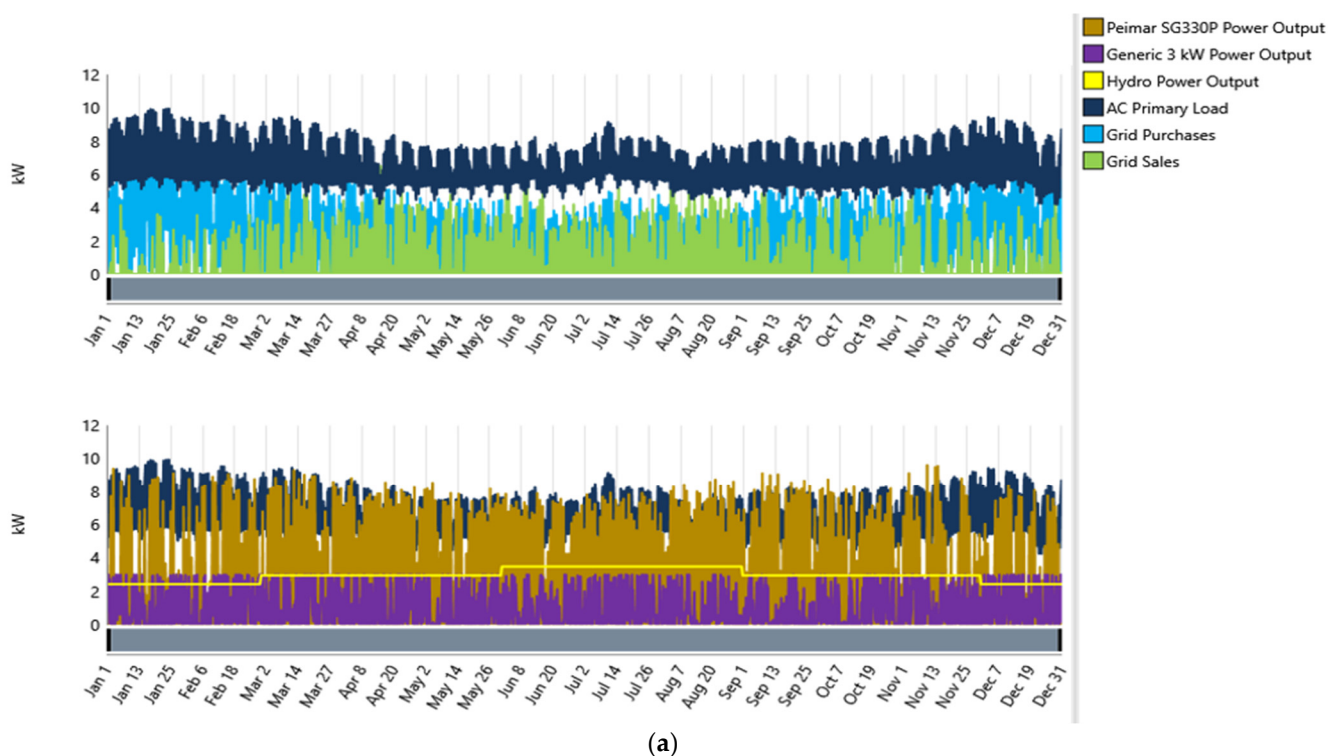


Figure 17. Electricity production with different components of the microgrid for the valves: (a) MP-02.5A-1, (b) SM04.5B, (c) TR08B.

All energy systems are integrated into the microgrid system with the valve MP-02.5A-1 to cover the energy demand. On the other hand, in the case of valve SM04.5B with a flow rate of 43.12 L/s, the wind turbine is excluded from the configuration due to the higher energy production of the PAT’s hydro power, which has a more favorable LCOE. In particular, in the case of valve TR08B, with a flow rate of 152.41 L/s, only the PAT (hydro power) is used since it is sufficient to meet the power demand without additional power systems. The grid is used in all cases, as there is a possibility to export surplus electricity to the grid as well. The transition from excluding high-cost energy systems at the lowest flow value of hydropower to using PATs exclusively at the highest flow value underscores the importance of PATs as a cost-effective solution for small communities.

Figure 18a–c visually represent the power consumption within the microgrid energy system. These figures illustrate the operation of the microgrid system and the energy output of all the energy systems to meet the energy demand. The grid draws decrease as the water capacity increases. In the case of TR08B (Case 3), not only is the demand met, but excess energy is also generated, resulting in a negative net cost. The main objective of a microgrid is to reduce costs while ensuring continuous load demand coverage.



(a)

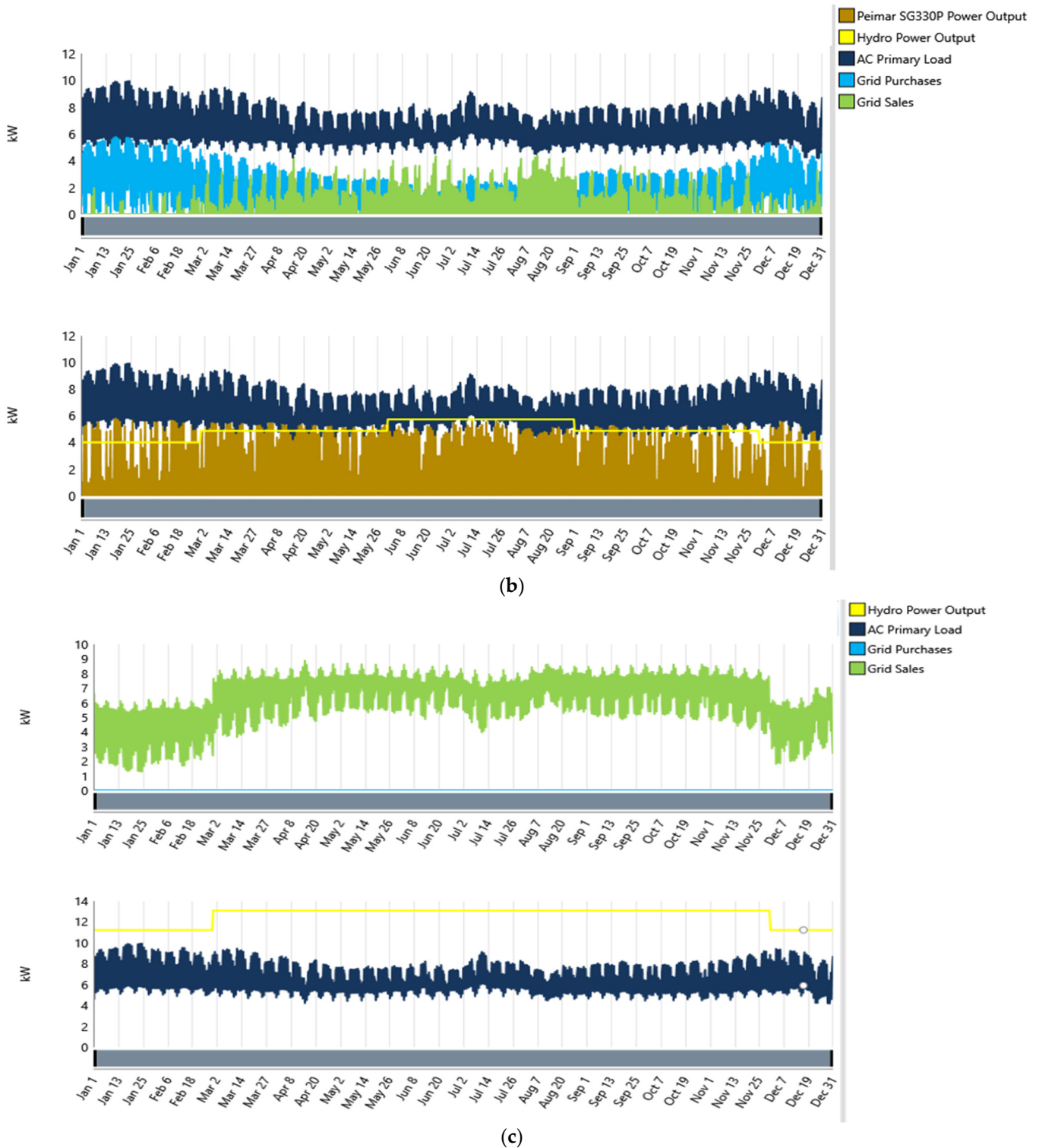


Figure 18. Meeting load demand with all the energy systems of the microgrid for the valves: (a) MP-02.5A-1, (b) SM04.5B, and (c) TR08B.

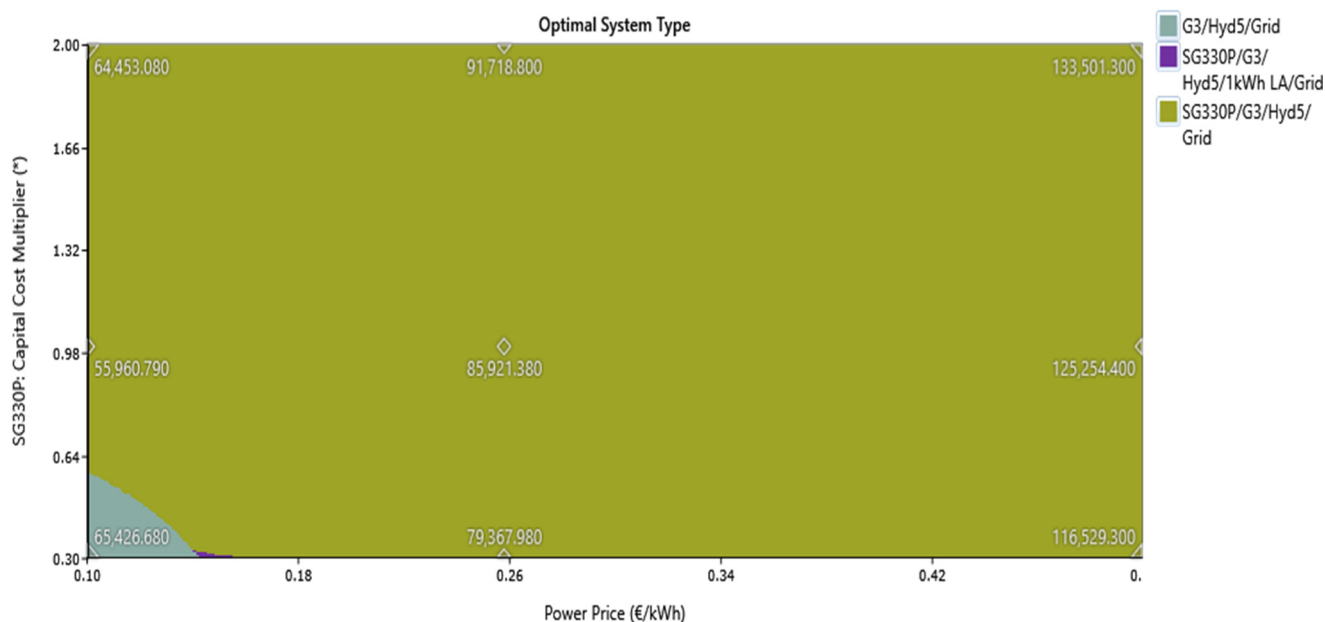
A sensitivity analysis was performed for the three selected cases to evaluate the variation in power system configurations. Figure 19a–c illustrate the optimal cost-effective solutions with varying capital costs for solar PV and a constant capital cost of 0.3 for the wind turbine. Notably, the wind turbine has the highest LCOE compared to the other power systems. The variations in grid purchase price were between 0.1 EUR/kWh and 0.5 EUR/kWh.

Considering all these variables, we see that hydropower remains a consistent component across all sensitivity cases, underscoring the indispensability of the pump as a turbine (PAT), even given the cost variations in solar PV, grid, and wind turbine. In the baseline case with the MP-02.5A-1 valve, a significant portion of the sensitivity spectrum is covered by the optimal combination of solar PV, wind turbine, hydropower, and grid. However, this dominance decreases in the case of valve SM04.5B, where the flow rate of the turbine is higher. This increase in flow rate leads to higher electricity generation from PATs, which have the lowest LCOE. Remarkably, the last case uses only hydropower, which consistently results in negative net cost (NPC). This is due to the sufficient hydropower generation that not only meets the load demand but also generates a surplus of electricity that exceeds the installation cost due to the revenue from grid recovery.

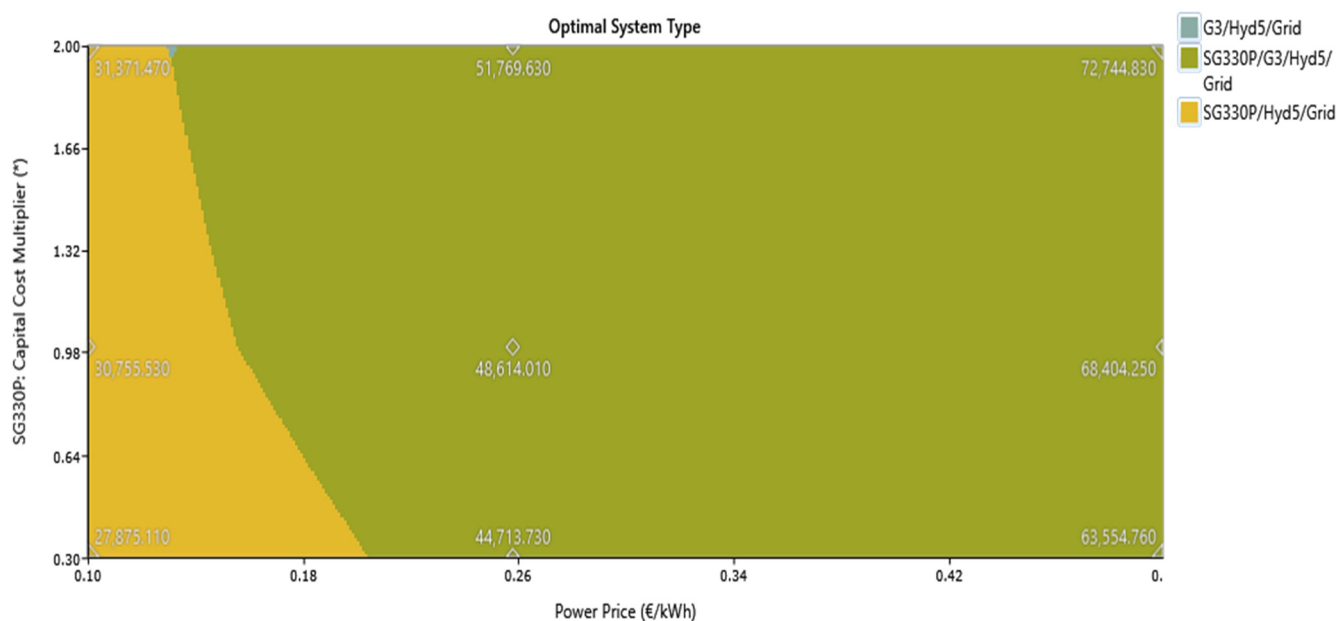
The sensitivity analysis, which includes variations in photovoltaic, wind turbine, and grid purchase costs within the specified range, consistently emphasizes the need to include hydropower in all conceivable energy systems to achieve the lowest NPC for meeting load demand. Through this sensitivity analysis, it can be conclusively stated that PATs are a cost-effective approach to small-scale renewable energy.

It is essential to note that this study is based on estimated averages for the different seasons. In addition, the limitations of HOMER, which restrict the inclusion of multiple hydro turbines, mean that this study cannot explore the full potential of multiple PATs within a microgrid system. Nonetheless, alternative tools can be used to explore the full integration of PATs in such systems.

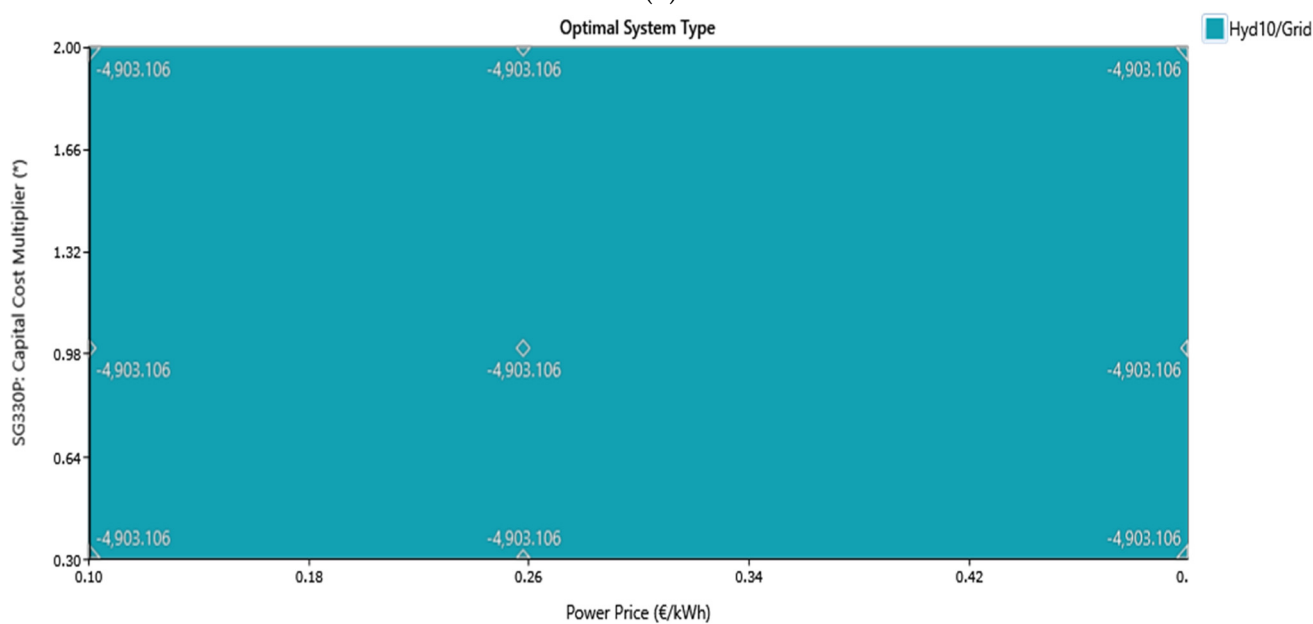
In summary, all of the simulations of HOMER in the various cases and scenarios aimed to satisfy electricity demand through selected small energy community systems, and while these systems may vary depending on the load size, hydropower remains a central component for cost-effective power generation throughout.



(a)



(b)



(c)

Figure 19. Sensitivity analysis with wind turbine capital cost multiplier of 0.3 for the valve: (a) MP-02.5A-1, (b) SM04.5B, (c) TR08B.

This research paves the way for future studies in smart cities and in various small energy communities (i.e., topographic features, flow and drop heights, solar radiation and wind availability, and type of turbines) where sophisticated systems can be deployed to harness energy from PATs for integration into the microgrid. These future studies could also include demand forecasting based on weather patterns and components that influence electricity prices and promise economic benefits and opportunities in distributed renewable generation.

4. Conclusions

The world’s water supply systems face high energy consumption and water loss due to poor management and inadequate water utility practices. Frequent breaks and leaks in

these networks are associated with inadequate water pressure regulation, which reduces system efficiency and increases demand for water and energy. This mismanagement strains water and energy resources, which are critical in today's society and environmental context, especially with the increasing threat of climate change and population growth exacerbating water scarcity. Addressing water losses and energy inefficiencies is essential for sustainable development without compromising the quality of life of future generations.

A new optimized method is proposed to achieve the following:

- Integrate micro-hydropower plants into water distribution systems, creating hybrid energy solutions.
- Replace or add pressure control valves with PATs, allowing for clean power generation while maintaining pressure levels within certain limits.
- Apply a real case study for an alternative solution, using the Funchal water network as an ideal case study for implementing this energy recovery method.
- Demonstrate suitable locations for pressure-reducing valves (PRVs) and for the implementation of PATs.
- A comprehensive analysis of the system's operation to evaluate the economic feasibility of the investment.

A simulation model for hydraulics developed by EPA, USA (EPANET), and for energy systems developed by the National Renewable Energy Laboratory in the USA (HOMER Pro) were used. This study uses the model to analyze the economic benefits of using pumps as turbines (PATs) for small-scale power generation and to gain insights into how microgrids can meet energy demand with PATs. Sensitivity analysis is performed to evaluate the variability of the microgrid system in response to variations in the cost of its energy components. The economic analysis shows favorable results for integrating PATs with a positive net present value (NPV). The highest NPV was obtained for the TR08B valve with a maximum flow rate of 152.41 L/s. The grid-connected microgrid system includes PV solar, wind turbines, and hydropower. The sensitivity analysis results consistently show the economic viability of PATs under different scenarios, even when the costs of PV, wind turbines, and grid infrastructure are reduced.

In all simulation cases, PATs have the lowest electricity (LCOE) cost compared to other energy systems, confirming their economic feasibility and efficiency. Based on the comprehensive methodology developed, it is clear that pumps as turbines (PATs) occupy a central role in cost-effective small-scale power generation. Consequently, many PATs have emerged as alternatives to conventional turbines due to their cost-effectiveness, accessibility, and reasonable efficiency. To evaluate the feasibility of this technology, the water distribution system in Funchal, Portugal served as a case study for implementing several PATs in conjunction with pressure-reducing valves (PRVs) at sites with significant energy recovery potential. The following are the main conclusions from this part:

- i. Variable-speed electrical regulation (ER) is preferable to a fixed-speed ER because it provides slightly higher performance for the exact equipment cost.
- ii. The "no regulation" mode (NR) is an unsuitable investment because it cannot adapt to fluctuating flow conditions, resulting in limited energy output.
- iii. Of the 50 newly implemented PRVs in Funchal's water distribution system, only 10 PRVs were deemed viable for PAT. These PRVs together generate 406 MWh/year of energy, with a combined net present value.

Hydraulic analysis shows significant potential for hydroelectric generation, especially in small communities where favorable topographic conditions for power generation in inclined grids lead to promising economic and energy results. This also contributes to positive environmental impacts by promoting the sustainability of water distribution.

In energy analysis, the HOMER model, used by professionals in over 150 countries for microgrid projects, provides optimized solutions that achieve the lowest net present cost (NPC) while meeting load demand. The main objective of using this model in research

is to highlight the importance of PATs in achieving economic benefits from small-scale power generation. Key findings from this part of the analysis include the following:

- i. Various PRVs were identified, and simulations were performed for each local system without changing the load and other power system specifications, such as capital, O&M, and replacement costs.
- ii. All simulations for all valves resulted in positive net present values, and additional analyses were performed to understand the nature of the economic benefits resulting from increased electricity generation from micro-hydro using PATs.
- iii. PV solar and micro-wind turbines installed in small DMAs in Funchal's water distribution system produce 153 MWh/year and 55 MWh/year, respectively, adding to the 406 MWh/year generated by PATs. This adds up to 615 MWh/year at the ten selected PRV sites within Funchal's water network alone.

In addition, the sensitivity analysis shows that the inclusion of PATs remains a cost-effective solution for various scenarios with capital cost multipliers for solar PV, wind, and grid purchase costs. This methodology currently considers the inclusion of a hydro turbine for the simulations. Future research incorporating multiple PATs will provide deeper insights into the different types of microgrid behavior in smart cities and communities. The integration of the micro-hydropower systems could contribute with other clean energy systems to achieve having zero non-renewable resources in the water cycle.

Author Contributions: Conceptualization, H.M.R. and P.S.M.G.; methodology A.K., H.M.R. and M.P.-S.; software P.S.M.G. and O.E.C.-H.; validation, A.C. and H.M.R.; formal analysis, H.M.R., M.P.-S., J.F.P.F. and P.J.C.B.; supervision, H.M.R. and P.A.L.-J. All authors have read and agreed to the published version of the manuscript.

Funding: This research was supported by Foundation for Science and Technology of Portugal, grant number UIDB/04625/2020; HY4RES—Hybrid solutions for Renewable Energy Systems: achieving net-zero Atlantic area energy consumers & communities, Interreg project EAPA_0001/2022; and Spanish State Research Plan Scientific and Technical and Innovation 2017–2020 PID2020-114781RA-I00.

Data Availability Statement: Data will be available when readers request to authors

Acknowledgments: The authors would like to thank CERIS for the funding support through the Foundation for Science and Technology of Portugal, through the funding UIDB/04625/2020, and to RSS—redes e sistemas de saneamento lda, rss@netcabo.pt for the data sources and analyses. This research was also partly developed along the research stay of the corresponding author called "The improvement of the energy efficiency in water systems using micro-hydropower systems and other renewable systems".

Conflicts of Interest: The authors declare no conflicts of interest.

References

1. Sun, X.; Zhu, B.K.; Zhang, S.; Zeng, H.; Li, K.; Wang, B.; Dong, Z.F.; Zhou, C.C. New indices system for quantifying the nexus between economic-social development, natural resources consumption, and environmental pollution in China during 1978–2018. *Sci. Total Environ.* **2022**, *804*, 150180. <https://doi.org/10.1016/j.scitotenv.2021.150180>.
2. Chau, K.Y.; Moslehpour, M.; Tu, Y.T.; Tai, N.T.; Tien, N.H.; Huy, P.Q. Exploring the impact of green energy and consumption on the sustainability of natural resources: Empirical evidence from G7 countries. *Renew. Energy* **2022**, *196*, 1241–1249. <https://doi.org/10.1016/j.renene.2022.07.085>.
3. Guo, Y.; Uhde, H.; Wen, W. Uncertainty of energy consumption and CO₂ emissions in the building sector in China. *Sustain. Cities Soc.* **2023**, *97*, 104728. <https://doi.org/10.1016/j.scs.2023.104728>.
4. Sandri, S.; Hussein, H.; Alshyab, N. Sustainability of the Energy Sector in Jordan: Challenges and Opportunities. *Sustainability* **2020**, *12*, 10465. <https://doi.org/10.3390/su122410465>.
5. Oberascher, M.; Rauch, W.; Sitzenfrei, R. Towards a smart water city: A comprehensive review of applications, data requirements, and communication technologies for integrated management. *Sustain. Cities Soc.* **2022**, *76*, 103442. <https://doi.org/10.1016/j.scs.2021.103442>.
6. Pahl-Wostl, C.; Vörösmarty, C.; Bhaduri, A.; Bogardi, J.; Rockström, J.; Alcamo, J. Towards a sustainable water future: Shaping the next decade of global water research. *Curr. Opin. Environ. Sustain.* **2013**, *5*, 708–714.

7. Russo, T.; Alfredo, K.; Fisher, J. Sustainable water management in urban, agricultural, and natural systems. *Water* **2014**, *6*, 3934–3956.
8. Wakeel, M.; Chen, B.; Hayat, T.; Alsaedi, A.; Ahmad, B. Energy consumption for water use cycles in different countries: A review. *Appl. Energy* **2016**, *178*, 868–885. <https://doi.org/10.1016/j.apenergy.2016.06.114>.
9. Luderer, G.; Madeddu, S.; Merfort, L.; Ueckerdt, F.; Pehl, M.; Pietzcker, R.; Rottoli, M.; Schreyer, F.; Bauer, N.; Baumstark, L.; et al. Impact of declining renewable energy costs on electrification in low-emission scenarios. *Nat. Energy* **2022**, *7*, 32–42. <https://doi.org/10.1038/s41560-021-00937-z>.
10. Sawle, Y.; Gupta, S.C.; Bohre, A.K. Review of hybrid renewable energy systems with comparative analysis of off-grid hybrid system. *Renew. Sustain. Energy Rev.* **2018**, *81*, 2217–2235. <https://doi.org/10.1016/j.rser.2017.06.033>.
11. Javed, M.S.; Zhong, D.; Ma, T.; Song, A.; Ahmed, S. Hybrid pumped hydro and battery storage for renewable energy based power supply system. *Appl. Energy* **2020**, *257*, 114026. <https://doi.org/10.1016/j.apenergy.2019.114026>.
12. Das, P.; Das, B.K.; Mustafi, N.N.; Sakir, M.T. A review on pump-hydro storage for renewable and hybrid energy systems applications. *Energy Storage* **2021**, *3*, e223.
13. Erdinc, O.; Uzunoglu, M. Optimum design of hybrid renewable energy systems: Overview of different approaches. *Renew. Sustain. Energy Rev.* **2012**, *16*, 1412–1425. <https://doi.org/10.1016/j.rser.2011.11.011>.
14. Khatib, T.; Mohamed, A.; Sopian, K. A review of photovoltaic systems size optimization techniques. *Renew. Sustain. Energy Rev.* **2013**, *22*, 454–465. <https://doi.org/10.1016/j.rser.2013.02.023>.
15. Baños, R.; Manzano-Agugliaro, F.; Montoya, F.G.; Gil, C.; Alcayde, A.; Gómez, J. Optimization methods applied to renewable and sustainable energy: A review. *Renew. Sustain. Energy Rev.* **2011**, *15*, 1753–1766. <https://doi.org/10.1016/j.rser.2010.12.008>.
16. Chan, A.L.S. Generation of typical meteorological years using genetic algorithm for different energy systems. *Renew. Energy* **2016**, *90*, 1–13. <https://doi.org/10.1016/j.renene.2015.12.052>.
17. Lorestani, A.; Ardehali, M.M. Optimization of autonomous combined heat and power system including PVT, WT, storages, and electric heat utilizing novel evolutionary particle swarm optimization algorithm. *Renew. Energy* **2018**, *119*, 490–503. <https://doi.org/10.1016/j.renene.2017.12.037>.
18. Moosavian, S.M.; Modiri-Delshad, M.; Rahim, N.A.; Selvaraj, J. Imperialistic competition algorithm: Novel advanced approach to optimal sizing of hybrid power system. *J. Renew. Sustain. Energy* **2013**, *5*, 053141. <https://doi.org/10.1063/1.4824977>.
19. Dehghan, S.; Kiani, B.; Kazemi, A.; Parizad, A. Optimal sizing of a hybrid wind/PV plant considering reliability indices. *World Acad. Sci. Eng. Technol.* **2009**, *56*, 527–535.
20. Askarzadeh, A. Distribution generation by photovoltaic and diesel generator systems: Energy management and size optimization by a new approach for a stand-alone application. *Energy* **2017**, *122*, 542–551. <https://doi.org/10.1016/j.energy.2017.01.105>.
21. Hadidian-Moghaddam, M.J.; Arabi-Nowdeh, S.; Bigdeli, M. Optimal sizing of a stand-alone hybrid photovoltaic/wind system using new grey Wolf optimizer considering reliability. *J. Renew. Sustain. Energy* **2016**, *8*, 035903. <https://doi.org/10.1063/1.4950945>.
22. Kaabeche, A.; Diaf, S.; Ibtouen, R. Firefly-inspired algorithm for optimal sizing of renewable hybrid system considering reliability criteria. *Sol. Energy* **2017**, *155*, 727–738. <https://doi.org/10.1016/j.solener.2017.06.070>.
23. Maleki, A.; Pourfayaz, F.; Rosen, M.A. A novel framework for optimal design of hybrid renewable energy-based autonomous energy systems: A case study for Namin, Iran. *Energy* **2016**, *98*, 168–180. <https://doi.org/10.1016/j.energy.2015.12.133>.
24. Maleki, A.; Pourfayaz, F. Optimal sizing of autonomous hybrid photovoltaic/wind/battery power system with LPSP technology by using evolutionary algorithms. *Sol. Energy* **2015**, *115*, 471–483. <https://doi.org/10.1016/j.solener.2015.03.004>.
25. Maleki, A.; Askarzadeh, A. Artificial bee swarm optimization for optimum sizing of a stand-alone PV/WT/FC hybrid system considering LPSP concept. *Sol. Energy* **2014**, *107*, 227–235. <https://doi.org/10.1016/j.solener.2014.05.016>.
26. Sedighzadeh, M.; Esmaili, M.; Esmaeili, M. Application of the hybrid Big Bang-Big Crunch algorithm to optimal reconfiguration and distributed generation power allocation in distribution systems. *Energy* **2014**, *76*, 920–930. <https://doi.org/10.1016/j.energy.2014.09.004>.
27. Shezan, S.K.A.; Julai, S.; Kibria, M.A.; Ullah, K.R.; Saidur, R.; Chong, W.T.; Akikur, R.K. Performance analysis of an off-grid wind-PV (photovoltaic)-diesel-battery hybrid energy system feasible for remote areas. *J. Clean. Prod.* **2016**, *125*, 121–132. <https://doi.org/10.1016/j.jclepro.2016.03.014>.
28. Ramos, H.M.; Zilhao, M.; López-Jiménez, P.A.; Pérez-Sánchez, M. Sustainable water-energy nexus in the optimization of the BBC golf-course using renewable energies. *Urban Water J.* **2019**, *16*, 215–224. <https://doi.org/10.1080/1573062X.2019.1648529>.
29. Mercedes Garcia, A.V.; Sánchez-Romero, F.J.; López-Jiménez, P.A.; Pérez-Sánchez, M. A new optimization approach for the use of hybrid renewable systems in the search of the zero net energy consumption in water irrigation systems. *Renew. Energy* **2022**, *195*, 853–871. <https://doi.org/10.1016/j.renene.2022.06.060>.
30. García, A.V.M.; Sánchez-Romero, F.-J.; López-Jiménez, P.A.; Pérez-Sánchez, M. Is it possible to develop a green management strategy applied to water systems in isolated cities? An optimized case study in the Bahamas. *Sustain. Cities Soc.* **2022**, *85*, 104093. <https://doi.org/10.1016/j.scs.2022.104093>.
31. Sowby, R.B. Correlation of Energy Management Policies with Lower Energy Use in Public Water Systems. *J. Water Resour. Plan. Manag.* **2018**, *144*, 06018007. [https://doi.org/10.1061/\(asce\)wr.1943-5452.0001006](https://doi.org/10.1061/(asce)wr.1943-5452.0001006).
32. Wu, D.; Fan, G.; Duan, Y.; Liu, A.; Zhang, P.; Guo, J.; Lin, C. Collaborative optimization method and energy-saving, carbon-abatement potential evaluation for nearly-zero energy community supply system with different scenarios. *Sustain. Cities Soc.* **2023**, *91*, 104428. <https://doi.org/10.1016/j.scs.2023.104428>.

33. Lode, M.L.; Felice, A.; Martinez Alonso, A.; De Silva, J.; Angulo, M.E.; Lowitzsch, J.; Coosemans, T.; Ramirez Camargo, L. Energy communities in rural areas: The participatory case study of Vega de Valcarce, Spain. *Renew. Energy* **2023**, *216*, 119030. <https://doi.org/10.1016/j.renene.2023.119030>.
34. Dorahaki, S.; Rashidinejad, M.; MollahassaniPour, M.; Pourakbari Kasmaei, M.; Afzali, P. A sharing economy model for a sustainable community energy storage considering end-user comfort. *Sustain. Cities Soc.* **2023**, *97*, 104786. <https://doi.org/10.1016/j.scs.2023.104786>.
35. Laske, S.; Paudel, A.; Scheibelhofer, O.; Sacher, S.; Hoermann, T.; Khinast, J.; Kelly, A.; Rantannen, J.; Korhonen, O.; Stauffer, F.; et al. A review of PAT strategies in secondary solid oral dosage manufacturing of small molecules. *J. Pharm. Sci.* **2017**, *106*, 667–712.
36. Novara, D.; Fecarotta, O.; Carravetta, A.; Derakhshan, S.; McNabola, A.; Ramos, H.M. Pumps as Turbines (PATs) Cost Determination and Feasibility Study of Pressure Reducing Valve Substitution or Replacement with a PAT in a Water Supply System. 2016. Available online: <https://www.semanticscholar.org/paper/Cost-Model-for-Pumps-as-Turbines-in-Run-of-River-Novara-Carravetta/4fd88f3e3444f22ca4bd0ed700772312d1c2fb96> (accessed on 16 January 2024).
37. Alberizzi, J.C.; Renzi, M.; Righetti, M.; Pisaturo, G.R.; Rossi, M. Speed and pressure controls of pumps-as-turbines installed in branch of water-distribution network subjected to highly variable flow rates. *Energies* **2019**, *12*, 4738.
38. Carravetta, A.; Fecarotta, O.; Del Giudic, G.; Ramos, H. Energy recovery in water systems by PATs: A comparisons among the different installation schemes. *Procedia Eng.* **2014**, *70*, 275–284.
39. Nautiyal, H.; Varun; Kumar, A. Reverse running pumps analytical, experimental and computational study: A review. *Renew. Sustain. Energy Rev.* **2010**, *14*, 2059–2067.
40. Derakhshan, S.; Nourbakhsh, A. Experimental study of characteristic curves of centrifugal pumps working as turbines in different specific speeds. *Exp. Therm. Fluid Sci.* **2008**, *32*, 800–807.
41. Derakhshan, S.; Nourbakhsh, A. Theoretical, numerical and experimental investigation of centrifugal pumps in reverse operation. *Exp. Therm. Fluid Sci.* **2008**, *32*, 1620–1627.
42. Energy Market Information System. Available online: <https://mercado.ren.pt/EN/Gas/MarketInfo/Load/Actual/Pages/Hourly.aspx> (accessed on 10 April 2023).
43. Novara, D.; Carravetta, A.; McNabola, A.; Ramos, H.M. 'A Cost Model for Pumps as Turbines in Run-off-River and in-Pipe Micro-Hydropower Applications'. *J. Water Resour. Plan. Manag.* **2018**, *145*, 04019012. [https://doi.org/10.1061/\(ASCE\)WR.1943-5452.0001063](https://doi.org/10.1061/(ASCE)WR.1943-5452.0001063).
44. Ferreira, A.R. Energy Recovery in Water Distribution Networks towards Smart Water Grids. Master's Thesis, IST Instituto Superior Tecnico de Lisboa Lisboa, Lisbon, Portugal, 2017.
45. Chhipi-Shrestha, G.; Hewage, K.; Sadiq, R. Economic and energy efficiency of net-zero water communities: System dynamics analysis. *J. Sustain. Water Built Environ.* **2018**, *4*, 04018006.
46. Crosson, C.; Achilli, A.; Zuniga-Teran, A.A.; Mack, E.A.; Albrecht, T.; Shrestha, P.; Boccelli, D.L.; Cath, T.Y.; Daigger, G.T.; Duan, J.; et al. Net zero urban water from concept to applications: Integrating natural, built, and social systems for responsive and adaptive solutions. *ACS ES&T Water* **2020**, *1*, 518–529.
47. Joustra, C.M.; Yeh, D.H. Framework for net-zero and net-positive building water cycle management. *Build. Res. Inf.* **2015**, *43*, 121–132.
48. Koirala, B.P.; Koliou, E.; Friegle, J.; Hakvoort, R.A.; Herder, P.M. Energetic communities for community energy: A review of key issues and trends shaping integrated community energy systems. *Renew. Sustain. Energy Rev.* **2016**, *56*, 722–744.
49. Lowitzsch, J.; Hoicka, C.E.; van Tulder, F.J. Renewable energy communities under the 2019 European Clean Energy Package—Governance model for the energy clusters of the future? *Renew. Sustain. Energy Rev.* **2020**, *122*, 109489.
50. Zhang, C.Y.; Oki, T. Water pricing reform for sustainable water resources management in China's agricultural sector. *Agric. Water Manag.* **2023**, *275*, 108045.

Disclaimer/Publisher's Note: The statements, opinions and data contained in all publications are solely those of the individual author(s) and contributor(s) and not of MDPI and/or the editor(s). MDPI and/or the editor(s) disclaim responsibility for any injury to people or property resulting from any ideas, methods, instructions or products referred to in the content.